

The effect of Dolutegravir on redox and vascular integrity

by

Janica Conradie



*Thesis presented in fulfilment of the requirements for the degree of
MSc in Clinical Pharmacology in the Faculty of Medicine and Health Sciences
at Stellenbosch University*

Supervisor: Professor Carine Smith

Co-supervisor: Dr Tracey Ollewagen

December 2022

Declaration

By submitting this thesis electronically, I declare that the entirety of the work contained therein is my own, original work, that I am the sole author thereof (save to the extent explicitly otherwise stated), that reproduction and publication thereof by Stellenbosch University will not infringe any third party rights and that I have not previously in its entirety or in part submitted it for obtaining any qualification.

December 2022

Copyright © 2022 Stellenbosch University
All rights reserved

Abstract

Background: Of the estimated 7.2 million people living with HIV (PLWH) in South Africa, more than 50% are on antiretroviral (ARV) medication. Dolutegravir (DTG), an integrase strand transfer inhibitor (INSTI), is increasingly used in South Africa (and Africa) as one of the first line treatments for HIV. Both *in vitro* and clinical studies indicate that DTG-based therapies have been associated with adverse effects (such as abnormal weight gain, hyperglycemia, and neurological dysfunction) alongside increased oxidative stress. Another disease state common in the South African context is obesity. DTG is administered to an individual regardless of their weight. As obesity is also associated with oxidative stress and inflammation, this might be a potential confounding factor in the efficacy and safety of DTG treatment. Endothelial dysfunction is one of the most common risk factors associated with non-communicable disease (such as obesity and CVD) and would therefore be an important phenomenon to investigate in the context of ARVs and obesity.

Aim: This study aimed to elucidate potential effects of chronic DTG on redox profile and endothelial integrity in the presence or absence of overfeeding as a confounder.

Methods: Adult zebrafish were subjected to chronic administration of DTG in the absence and presence of obesity (overfeeding model) over a period of 2 weeks. The lean zebrafish received Hikari dry pellets twice per day, whereas the overfed fish received the same food, six times per day over 4 weeks. A parallel 12-week DTG administration study was also executed in lean male and female Wistar rats. Body mass, reactive oxygen species (ROS) levels (hydrogen peroxide (H₂O₂)) and vascular endothelial tight junctions (claudin-5 and ZO-1) and adherens junction (VE-Cadherin) protein profile were evaluated.

Results: DTG did not have a significant effect on the body mass of adult zebrafish or rats. DTG administration showed no detrimental effect on ROS levels in either zebrafish or rats. When considering the effect of DTG on the expression of tight and adherens junction proteins, DTG showed no effect on the expression of ZO-1 and Claudin-5 in both zebrafish and rats. In terms of obesity, the overfed zebrafish had significantly higher body mass when compared to lean fish confirming successful execution of the overfeeding protocol. Overfeeding did not impact ROS, however there was a decrease in VE-cadherin expression in the zebrafish dorsal aorta, pointing to a cumulative effect of DTG and obesity (overfeeding).

Conclusion: This study suggests that in the absence of HIV, DTG does not have an effect on redox status and endothelial dysfunction in terms of tight and adherens junction integrity. However, the addition of overfeeding highlighted the cumulative effect of DTG and obesity on endothelial function, an effect that can potentially impact the human population.

Uittreksel

Agtergrond: Van die geraamde 7,2 miljoen mense wat met Menslike Immuniteitsgebrekswirus (MIV) in Suid-Afrika leef, gebruik meer as 50% antiretrovirale (ARV) medikasie. Dolutegravir (DTG) word toenemend in Suid-Afrika (en Afrika) gebruik as een van die eerste-lyn-behandelings vir MIV. Beide *in vitro* en kliniese studies dui daarop dat DTG-gebaseerde terapieë geassosieer word met nadelige kliniese effekte (soos gewigstoename, hiperglukemie en neurologiese disfunksie) en verhoogde oksidatiewe stres. Nog 'n siektetoestand wat algemeen voorkom in die Suid-Afrikaanse konteks, is vetsug. DTG word aan 'n individu toegedien ongeag hul gewig. Aangesien vetsug ook geassosieer word met oksidatiewe stres en inflammasie, kan dit 'n potensiële verwarrende faktor wees in die doeltreffendheid en veiligheid van DTG-behandeling. Endoteeldisfunksie is een van die mees algemene risikofaktore wat geassosieer word met nie-oordraagbare siektes (soos vetsug en kardiovaskulêre siekte) en sal dus 'n belangrike faktor wees om in die konteks van ARVs en vetsug te ondersoek.

Doel: Hierdie studie het uitgesit om die potensiële effekte van chroniese DTG op redoksprofiel en endoteelintegriteit in die teenwoordigheid of afwesigheid van oorvoeding as 'n versteurder toe uit te lig.

Metodes: Volwasse zebravisse is oor 'n tydperk van 2 weke aan chroniese toediening van DTG in die afwesigheid en teenwoordigheid van vetsug (oorvoedingsmodel) onderwerp. Die maer (kontrole) zebravisse het Hikari-vis-korrels twee keer per dag ontvang, terwyl die oorgevoerde visse ses keer per dag dieselfde kos ontvang het, vir 'n periode van 4 weke. 'n Parallele 12-week DTG administrasie studie is ook uitgevoer in maer manlike en vroulike Wistar rotte. Liggaamsmassa, reaktiewe suurstof spesies (ROS) vlakke (waterstofperoksied (H_2O_2) en vaskulêre endoteel stywe aansluitings (claudin-5 en ZO-1) en adherens aansluiting (VE-Cadherin) proteïenprofiel is geëvalueer.

Resultate: DTG het nie 'n betekenisvolle effek op die liggaamsmassa van volwasse zebravisse of rotte gehad nie. DTG-toediening het geen nadelige effek op ROS-vlakke in óf zebravisse óf rotte getoon nie. Wanneer die effek van DTG op die uitdrukking van stywe en adherens-verbindingsproteïene oorweeg is, het DTG geen effek op die uitdrukking van ZO-1 en claudin-5 in beide zebravisse en rotte getoon nie. Wat vetsug betref, het die oorvoede zebravis aansienlik hoër liggaamsmassa getoon in vergelyking met maer vis wat die suksesvolle uitvoering van die oorvoedingsprotokol bevestig. Oorvoeding het nie ROS beïnvloed nie, maar daar was 'n afname in VE-cadherin uitdrukking in die zebravis dorsale aorta, wat dui op 'n kumulatiewe effek van DTG en vetsug (oorvoeding).

Gevolgtrekking: Hierdie studie dui daarop dat in die afwesigheid van MIV, DTG nie 'n effek op redoksstatus en endoteeldisfunksie het in terme van stywe en adherens aansluiting integriteit nie. Die byvoeging van oorvoeding het egter die kumulatiewe effek van DTG en vetsug op endoteelfunksie uitgelig, 'n effek wat potensiëel die menslike bevolking kan beïnvloed.

Acknowledgements

Firstly, I would like to thank Prof Carine Smith, my supervisor for her endless support, encouragement and guidance. Then, I would like to thank The Clinical Pharmacology department for all of the help and support and the NHLS at Tygerberg Hospital for their assistance and the use of their equipment.

I would like to thank my family and friends for all of their love and support throughout my thesis. Dankie DeWalt, vir jou nimmereindigende ondersteuning!. Dankie aan my pa, Alewyn wat my #1 supporter is.

Finally, thank you to Tracey Ollewagen, my co-supervisor and mentor. Words can't explain what you have taught me and what you mean to me.

Table of Contents

1. INTRODUCTION	1
2. LITERATURE REVIEW.....	3
2.1. Introduction.....	3
2.2. Antiretroviral treatment	4
2.2.1. Focus on Dolutegravir	5
2.3. Endothelial function and redox: inextricably linked.....	11
2.3.1. Redox and endothelial dysregulation in the context of DTG and obesity	15
2.4. Significance of obesity as potential confounder	19
2.4.1. Adipose dysregulation in obesity	20
2.5. Methodological considerations	22
2.5.1. Inclusion of both sexes	22
2.5.2. Choice of animal models.....	23
2.5.3. Inducing obesity in zebrafish.....	25
2.6. Rationale	26
2.7. Hypothesis statement.....	26
3. MATERIALS AND METHODS	28
3.1. Dolutegravir exposure in lean and overfed adult Zebrafish.....	28
3.1.1 Ethical considerations.....	28
3.1.2 Experimental groups and procedures.....	28
3.1.3 Overfeeding protocol.....	28
3.1.4 Dolutegravir administration	29
3.1.5 Sample collection	31
3.2. DTG exposure in rodent model.....	32
3.2.1. Ethical considerations.....	32
3.2.2. Experimental animals	32
3.2.3. Intervention: Dolutegravir administration.....	33
3.2.4. Sample collection	33

3.3. Sample analysis	34
3.3.1 Reactive oxygen species (ROS)	34
3.3.2. Histology and tight junction protein expression of the rat and zebrafish aorta	35
3.4. Statistical analysis	36
4. RESULTS	37
4.1. The adult zebrafish model	37
4.2. The rat model	45
5. DISCUSSION	50
5.1. The effects of Dolutegravir	50
5.2. The effects of Obesity as potential confounder	53
5.3. Comparison of zebrafish and rat models	54
5.4. Conclusion	55
6. REFERENCES	56
7. LIST OF APPENDICES	70
7.1. Appendix A	70
7.2. Appendix B	71
7.3. Appendix C	72

List of figures

Figure 2.1: Some of the factors and pathways responsible for HIV-associated CVD. CVD- cardiovascular diseases; ICAM-1- intercellular adhesion molecule 1; NO- nitric oxide; PAI-1- plasminogen activator inhibitor-1; TF - tissue factor; VCAM-1- vascular cell adhesion protein 1 (Dominick et al., 2020)	4
Figure 2.2: Tight junctions and adherens-junctions in the endothelium. VE-cadherin is linked to actin filaments via α - and β -catenin. Occludin and Claudin-5 is linked to the actin filaments via the interaction with ZO-1 (Biorender.com).	13
Figure 2.3: Inflammation and oxidative stress lead to endothelial damage though various mechanisms. Endothelial damage and lipid peroxidation are key risk factors for atherosclerosis. IL- Interleukin, MPO- Myeloperoxidase, NF-kB- nuclear factor-kB, NO- nitric oxide, LDL- low-density lipoprotein, ROS- reactive oxygen species, NADPH- nicotinamide adenine dinucleotide phosphate hydrogen, NO-nitric oxide.....	14
Figure 2.4: The effect of pro-inflammatory cytokines and adhesion molecules on the assembly and disassembly of the tight- and adherens junctions in the endothelial cells. Additionally, the transmigration of leukocytes is also depicted (from, Medina-Leyte et al., 2021).	17
Figure 2.5: Adipose tissue undergoing an inflammatory maladaptive response in obesity (adapted from Makki et al., 2013).....	20
Figure 2.6: The effect of oxidative stress in adipose tissue on other physiological pathways which may lead to other disease states (from Matsuda and Shimomura, 2013).	22
Figure 2.7: The development of the dorsal aorta from A) 7dpf to B) 1mpf and C) 3-month-old adult zebrafish. The aorta is depicted by the black arrow. From: (Miano et al., 2006).....	24
Figure 3.1: The overfeeding protocol used in the study. DF- Dry food.	29
Figure 3.2: Timeline of the adult zebrafish study.	30
Figure 3.3: The coating of the Hikari fish pellets with DTG.	31
Figure 3.4: The figure of how the body of zebrafish were harvested. The red arrow indicates the direction of sectioning for the dorsal aorta. The black arrow indicates the direction of sectioning for the brain and bulbous arteriosus.	32

- Figure 3.5:** The rat brain section used for this study (indicated by the red section). The left and right lobes were separated, and the right lobe was again cut in half, where this study used the innermost part of the brain. 34
- Figure 3.6:** The measurements set in ImageJ and an example of how the aortas were analysed for the different fluorescent proteins. 36
- Figure 4.1:** Representative images indicating the size of the adult zebrafish captured after euthanasia and weighing. The average length of an adult zebrafish is 2.9 cm ($\pm 0,2098$). The top row shows female zebrafish and the bottom row, male zebrafish. 37
- Figure 4.2:** Body mass (mg) of adult zebrafish comparing lean and obese groups. N=12 per group. Statistical analysis: unpaired t-test and Bonferroni post hoc test. Data represented as mean \pm SD. * = $p=0,0317$ 37
- Figure 4.3:** Body mass (mg) of adult zebrafish from the four different groups. N=12 per group. Statistical analysis: Kruskal-Wallis test and a Dunn's post hoc test. Data represented as mean \pm SD. DTG: Dolutegravir. 38
- Figure 4.4:** a) The body mass of the zebrafish per length (cm) and the b) BMI of the adult zebrafish. N=12 per group. Kruskal-Wallis test and Dunn's post hoc test. Data represented as mean \pm SD. $P < 0,05$ 39
- Figure 4.5:** H_2O_2 (mmol/L/10 mg/mL liver) measured from the adult zebrafish livers. Two livers were pooled, $n=3$ per group. Statistical analysis: One-way ANOVA and Bonferroni post hoc test. Data represented as mean \pm SD. DTG: Dolutegravir. 39
- Figure 4.6:** H&E stain of a transverse section of the a) adult zebrafish heart (scale bar: 100 μ m, magnification 10x plus the eyepiece magnification of 10x, total magnification: 100x)) and c) zebrafish brain, (scale bar: 50 μ m magnification 10x plus the eyepiece magnification of 10x, total magnification: 100x)) and fluorescence images of b) transverse section of the bulbus arteriosus of the zebrafish stained for claudin-5 (scale bar: 50 μ m, magnification 10x, plus the magnification of the eyepiece of 10x, thus total magnification of 100x) and d) transverse sections of the zebrafish brain stained for ZO-1 (scale bar: 50 μ m, magnification 10x, plus the magnification of the eyepiece of 10x, thus total magnification of 100x). Arrowheads indicate blood vessels, BA: Bulbus arteriosus CM: cardiac muscle. 41
- Figure 4.7:** H&E section of a transverse 10 μ m section of dorsal aorta of adult zebrafish (scale bar: 10 μ m, magnification 60x plus the eyepiece magnification of 10x, total magnification: 600x). Arrow: Red blood cells, T: Tubule of kidney. 42

- Figure 4.8:** Brightfield images demonstrated how the dorsal aorta was located, using the position of the brain (B) and the vertebra (V). Red arrow: Dorsal aorta. K: kidney tissue. Magnification: 4x, plus the magnification of the eyepiece 10x (total magnification is 40x). Scale bar represents 100 μ m. 42
- Figure 4.9:** Image analysis of tight and adherens junctions in adult zebrafish dorsal aorta. A) Representative images of Claudin 5, VE-cadherin and ZO-1 in the different groups. B) The mean fluorescence intensity (MFI) of the tight and adherens junction proteins assessed in adult zebrafish dorsal aorta. n=3 per group. Statistical analysis: One-way ANOVA and bonferonni post hoc and multiple t- test. Data are shown as the mean \pm SD. Magnification 10x plus 10x magnification of the eyepiece (total magnification 100x): Scale bar represents 50 μ m. Ψ : ANOVA main effect of treatment ($p < 0.05$). 45
- Figure 4.10:** The body mass of male and female Wistar rats over the period of the 12-week DTG study. Body mass were measured twice a week and depicted as such. DTG: Dolutegravir. 45
- Figure 4.11:** Body mass (g) of rats at the end of the study. N=6 per group. Statistical analysis: Two-way ANOVA and Bonferroni post hoc test. Data represented as mean \pm SD. ****= $p < 0.0001$. DTG: Dolutegravir. 46
- Figure 4.12:** The fasting blood glucose at the endpoint of the study. N=6 per group. Two-way ANOVA and Bonferroni post hoc test. Data represented as mean \pm SD. Ψ : Significant ANOVA effect on sex, $p = 0,0061$. DTG: Dolutegravir. 46
- Figure 4.13:** Rodent liver weight. a) The weights of the livers of the rats after harvesting and b) the weights of the livers corrected for body mass. N= 6 per group. Statistical analysis: Two-way ANOVA and Bonferroni post hoc test. Data represented as mean \pm SD. 47
- Figure 4.14:** The H₂O₂ (mmol/L/protein concentration) measured from the rat livers. N=6 per group. Statistical analysis: Two-way ANOVA and Bonferroni post hoc test. Data represented as mean \pm SD. Ψ : Significant ANOVA effect on sex, $p = 0,0026$ 47
- Figure 4.15:** H&E stain of a transverse section of the a) rat mid brain (scale bar: 200 μ m, magnification 4x plus the eyepiece magnification of 10x, total magnification: 40x) and b) fluorescence section of a c) rat aorta (scale bar: 100 μ m magnification 10x plus the eyepiece magnification of 10x, total magnification: 100x), Arrowhead: Blood vessel, Arrow: Hippocampal region of the brain. 48

Figure 4.16: Image analysis of tight and adherens junctions in the rat aorta. A) Representative images of Claudin 5, VE-cadherin and ZO-1 in the different groups. B) The mean fluorescence intensity (MFI) of the tight and adherens junction proteins assessed in rat aorta. n=3 per group. Statistical analysis: One-way ANOVA and Bonferroni post hoc test. Data represented as mean \pm SD. Magnification 10x plus 10x magnification of the eyepiece (total magnification 100x). Scale bar represents 50 μ m. 49

List of tables

Table 2.1: Side- effects of Dolutegravir. These are mostly reports from clinical settings.	7
Table 3.1: The values used to calculate the doses given to an individual adult zebrafish and rat, which is equivalent to the human dose.....	30
Table 3.2: Antibodies used for rat descending aorta and adult zebrafish dorsal aorta staining.	35
Table 7.1: The amount of the constituents found in Hikari micro pellets.....	72

List of abbreviations

ABC/3TC	Abacavir (Triumeq®) and Lamivudine
AT	Adipose tissue
ARV	Antiretroviral
ART	Antiretroviral therapy
ASC	Adipose stem cells
BAT	Brown adipose tissue
BB	Blocking buffer
BBB	Blood brain barrier
BMI	Body mass index
CVD	Cardiovascular disease
DTG	Dolutegravir
ETC	Electron transport chain
EVG	Elvitegravir
EVZ	Evafirenz
eNOS	Endothelial nitric oxide synthase
EtOH	Ethanol
FBS	Fetal bovine serum
FDA	Food and Drug Administration
H ₂ O ₂	Hydrogen peroxide
H&E	Haematoxylin and eosin
HAND	HIV-associated neurocognitive decline
HFD	High fat diet
HUVECs	Human vascular endothelial cells
ICAM-1	Intercellular adhesion molecule-2

INSTIs	Integrase strand transfer inhibitors
JAM	Junctional adhesion molecule
MetS	Metabolic syndrome
MFI	Mean fluorescence intensity
MHO	Metabolically healthy obesity
MUO	Metabolically unhealthy obesity
NADPH	Nicotinamide adenine dinucleotide phosphate
NFD	Normal fat diet
NF- κ B	Nuclear factor kappa B
NLRP	NOD-, LRR- and pyrin domain-containing protein
NNRTI	Non-nucleoside reverse transcriptase inhibitor
NO	Nitric oxide
Ox-LDL	Oxidized low density lipoprotein
PBS	Phosphate buffered saline
PECAM-1	Platelet endothelial cell adhesion molecule
PI	Protease inhibitor
PLWH	People living with HIV
PCAM-1	Platelet endothelial cell adhesion molecule-1
RAL	Raltegravir
ROS	Reactive oxygen species
SANS	South African National Standard
SD	Standard deviation
sICAM-1	Soluble intracellular cell adhesion molecule-1
SVF	Stromal vascular fraction
sVCAM-1	Soluble vascular cell adhesion molecule-1
TNF- α	Tumor-necrosis factor- α

Ve-PTP	Vascular endothelial cell protein tyrosine phosphatase
WAT	White adipose tissue
ZO-1	Zona occludens-1

CHAPTER 1

1. INTRODUCTION

Of the estimated 7.2 million people living with HIV (PLWH) in South Africa, more than 50% are on antiretroviral (ARV) medication. Research has highlighted the increased prevalence of cardiovascular risk factors, such as obesity, hyperglycaemia, hypertension, hypertriglyceridaemia, low high-density lipoprotein cholesterol (HDL-c), as well as atherosclerosis in PLWH receiving ARV treatment (Bavinger *et al.*, 2013; Dominick *et al.*, 2020; Nkeh-Chungag *et al.*, 2021). Moreover, the metabolic complications associated with HIV and ARVs (Nkeh-Chungag *et al.*, 2021) are a growing concern as it may result in increased risk of non-communicable diseases such as cardiovascular disease (CVD) and diabetes, in particular, in the South African population where there is a high prevalence of obesity (Alaba and Chola, 2014a) (WHO, 2016). Dolutegravir (DTG), an integrase strand transfer inhibitor (INSTI), is fast becoming the first line ARV strategy for the management of HIV in Africa.

DTG is utilized to decrease the viral load associated with HIV infection. It inhibits HIV integrase by binding to the active site and blocking the strand transfer step of retroviral RNA integration in the host cell - which is crucial in the HIV replication cycle – thus inhibiting viral activity. Unfortunately, INSTIs have recently been associated with increased weight gain when compared to protease inhibitor (PI)-based or non-nucleoside reverse transcriptase inhibitor (NNRTI)-based regimens (Eckard and McComsey, 2020). Moreover, DTG and Bictegravir, another INSTI, were both associated with greater weight gain than other drugs in the class of INSTIs (Sax *et al.*, 2020; Menard *et al.*, 2017; and Bourgi *et al.*, 2020). Other reported side effects of DTG such as hyperglycaemia (Hailu *et al.*, 2021; Hirigo *et al.*, 2022; Lamorde *et al.*, 2020; McLaughlin *et al.*, 2018), fat redistribution and neurological dysfunction (Hoffmann *et al.*, 2017) are equally disconcerting.

Given the high incidence of obesity in the South African population, these reported side effects of DTG are a significant cause for concern as it may exacerbate the already well-known detrimental effects of obesity on health. For example, obesity contributes to oxidative stress and inflammation, and metabolic dysregulation. Furthermore, relatively recent evidence suggests that adipocytes may harbour the HI-virus (Couturier *et al.*, 2018; Damouche *et al.*, 2015), thereby further increasing the risk to obese patients. Although DTG has demonstrated increased ability to penetrate adipose tissue when compared to non-integrase inhibitors (Couturier *et al.*, 2018), the effect of DTG on adipose redox and inflammatory status, via modulation of the secretory profiles of constituent cells, remains to be fully elucidated.

As oxidative stress and inflammation both are associated with DTG treatment and obesity, and since HIV-associated neurocognitive decline is linked to endothelial dysfunction (Gannon *et al.*, 2011; Schouten *et al.*, 2011), evaluation of potential endothelial dysfunction in both central and peripheral compartments in response to DTG treatment is warranted.

As some of the observed side-effects may also be ascribed to the HIV infection itself, additional pre-clinical models may allow for a more comprehensive analysis of the potential mechanisms of DTG in the absence of HIV. Therefore, the aim of this thesis was to investigate the effects that DTG has on endothelial integrity, in terms of tight-junction and adherens junction expression, in both non-obese and obese states. We also aimed to assess whether DTG administration affects redox status and if so, whether this is associated with vascular endothelial dysfunction.

CHAPTER 2

2. LITERATURE REVIEW

2.1. Introduction

The research on the association between HIV and CVD has grown substantially over the last decade and over the years more research strengthens this association. The literature is in agreement that HIV causes a chronic upregulation of inflammation in its host. Chronic inflammation has been one of the leading causes of CVD (Liu *et al.*, 2017) and may explain – at least in part - why HIV and CVD are linked. A review by Triant (2013) summarises evidence that HIV-associated inflammation and chronic immune activation (caused by immune dysregulation) are important factors in the development of CVD. ARV-naive HIV-positive patients have higher levels of soluble immune activation markers (such as pro-inflammatory cytokines (eg. Interleukin (IL)-6) and soluble adhesion leukocyte markers (eg. soluble vascular cell adhesion molecule (sVCAM-1)) when compared to non-HIV controls (Baker *et al.*, 2010). The association between HIV and CVD is confirmed by Dominick *et al.*, (2020) who describes that PLWH have a 61% greater chance at developing CVD opposed to those without HIV. They suggested that instead of looking at traditional risk factors for CVD and the side effects of ARVs, factors such as inflammation and persistent immune activation should be considered. As shown in Figure 2.1, Dominic *et al.* (2020) recently summarised the multiple factors and pathways responsible for the development of CVD in PLWH. This summary clearly points out the prominence of persistent immune activation and endothelial dysfunction in this context, but does not mention the role of oxidative damage, despite the interlinked nature of immune activation, inflammation and oxidative stress.

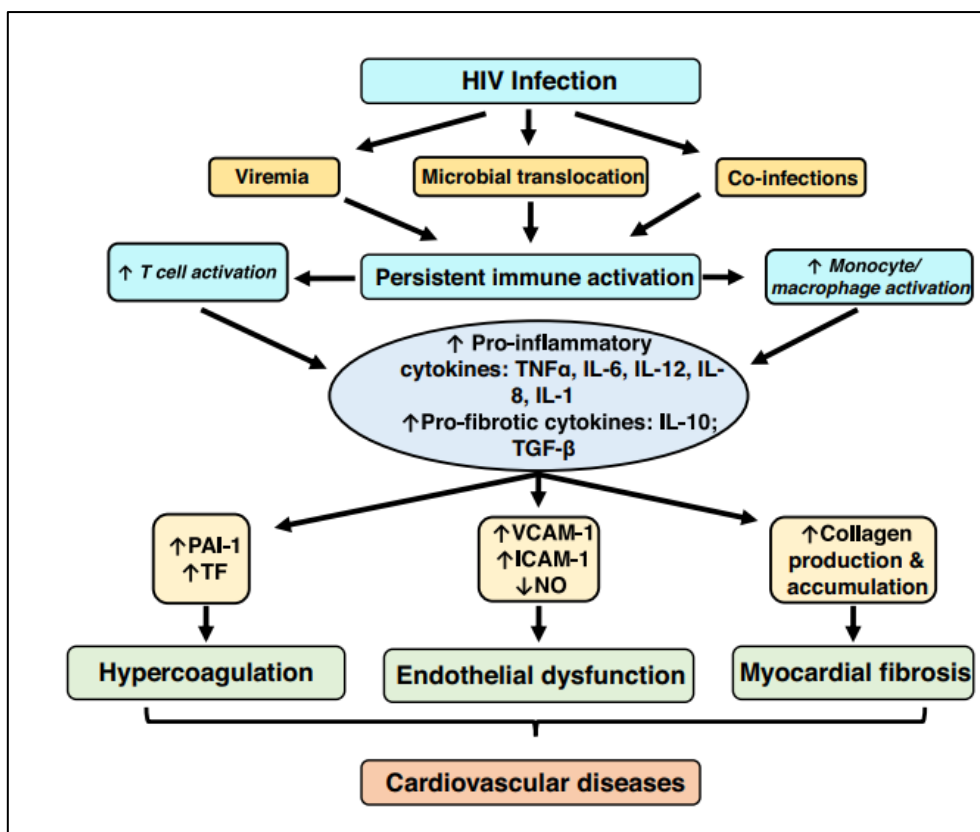


Figure 2.1: Some of the factors and pathways responsible for HIV-associated CVD. CVD- cardiovascular diseases; ICAM-1- intercellular adhesion molecule 1; NO- nitric oxide; PAI-1- plasminogen activator inhibitor-1; TF - tissue factor; VCAM-1- vascular cell adhesion protein 1 (Dominick et al., 2020)

The use of ARVs has become more prevalent, resulting in reduced impact of the side effects associated with HIV itself. However, the use of ARVs is also linked to adverse effects. For the purpose of this literature review, we will focus on two major aspects of ARV-associated adverse effects, namely endothelial health and redox status. The potential confounding effects of obesity in this context will also be included. However, in order to provide context, DTG as relatively new first-line ARV therapy (ART) will firstly be introduced, and a brief overview of side-effects reported for this drug will be provided.

2.2. Antiretroviral treatment

The introduction and increased use of ARVs has resulted in a dramatic decline in immunodeficiency related events, including deaths, in HIV-infected individuals (Trickey et al., 2017; World Health Organization, 2016).

Common ART regimens use a combination of three ARV agents with two modes of action. Nucleoside reverse transcriptase inhibitors (NRTIs) and NNRTIs block viral RNA transcription by inhibiting reverse transcriptase, PIs block viral enzyme protease and prevent the maturation of the virus, and integrase inhibitors - otherwise known as INSTIs - act against the viral DNA integration into the host genome (Kolakowska *et al.*, 2019).

Although ARVs have decreased the incidence of death among PLWH, there are a number of associated side effects linked with prolonged exposure of ARVs. In general, the side-effects reported in PLWH and/or patients receiving ART and specifically DTG, which include hypertension, weight gain, diabetes and dyslipidemia (de Boer *et al.*, 2016; Gorwood *et al.*, 2020; Hirigo *et al.*, 2022; Venter *et al.*, 2019), are similar to symptoms reported for metabolic syndrome (MetS) (Abraham *et al.*, 2013) and is in line with reported increased risk for the development of cardiovascular (Dominick *et al.*, 2020), lipid, immune, metabolic and neurological disorders, as well as cancer (Bertrand *et al.*, 2019; Grinspoon and Carr, 2005; Montenegro-Burke *et al.*, 2019a).

An exhaustive review of mechanisms responsible for side-effects reported after ARV use is outside the scope of this thesis. Rather, we will focus this review on the literature pertaining to side-effects (and potential causative mechanisms) reported in the context of DTG treatment specifically.

2.2.1. Focus on Dolutegravir

DTG, Raltegravir (RAL), and Elvitegravir (EVG) are integrase inhibitor ARVs. INSTIs specifically block/inhibit integrase, an enzyme necessary to integrate the viral RNA into the host's genome, therefore making the effects of integrase inhibitors highly specific (Kolakowska *et al.*, 2019). INSTI-based regimens have been recommended as initial therapy for many people diagnosed with HIV due to its low resistance profile (high barrier of resistance) (Kandel and Walmsley, 2015) and better tolerability.

DTG is a white/yellow pill, which is taken once daily. It is rapidly absorbed and has a half-life of 12 hours. As for the dosage, 50 mg of DTG was found the most effective in suppressing viral load in treatment naïve patients with the same amount of adverse effects as the lower doses (van Lunzen *et al.*, 2012).

DTG is mostly given as a combination therapy with Abacavir (Triumeq®) and Lamivudine (ABC/3TC)(NRTIS) (Hoffmann *et al.*, 2017). Other combinations are with Abacavir or Rilpivirine (Juluca®)(NNRTI) (Ma *et al.*, 2020). Most studies that has been presented with negative outcomes states that "DTG-based-therapies" caused the negative effect (Menard,

2017b; Zakumumpa *et al.*, 2021)). This is vague, and we cannot assume that those results portray the effects of DTG itself. It has been suggested that monotherapy of DTG is not recommended (Hocqueloux *et al.*, 2019) as monotherapy did not maintain virological suppression over time when compared to the combination therapy (DTG/ABC/3TC) and that the monotherapy showed signs of higher virological failure when compared to the combination therapy. This was confirmed by the DOMONO study (Wijting *et al.*, 2017), which indicates that the chances of only receiving DTG is unlikely.

A summary of the most often reported side-effects of dolutegravir can be found in Table 2.1.

Table 2.1: Side- effects of Dolutegravir. These are mostly reports from clinical settings.

Side effect	Suspected metabolic reason for side effect	Treatment protocol employed	Reference
Neuro-adverse effects/neurotoxicities (insomnia, headache, dizziness, depression etc.)	DTG has been found in high concentrations in the CNS.	50 mg of DTG once a day.	(Letendre <i>et al.</i> , 2014a)
	DTG has been found in high concentrations in the CNS.	Standard clinical treatment dose of DTG and single tablet regimen (STR) containing a combination of DTG, abacavir and lamivudine.	(Hoffmann <i>et al.</i> , 2017;)
	Proposed that DTG is able to cross the blood brain barrier.	50 mg of DTG once a day.	(Cahn <i>et al.</i> , 2013)
	None suggested	Standard treatment dose of DTG/abacavir/lamivudine.	(Correspondence to Menard, 2017)
Weight gain	None provided		(de Boer <i>et al.</i> , 2016)
	Confirmed, not a “return-to-health” phenomenon.	50 mg of DTG per day for 48 weeks.	(Venter <i>et al.</i> , 2019)

	<p>A rapid drop in viral load and the correlation of virologic suppression with lower energy expenditure.</p> <p><i>In vitro</i> DTG has been shown to affect the activity of melanocyte-stimulating hormone (involved in appetite control), which may explain increased weight gain due to increased appetite (Hill <i>et al.</i>, 2019).</p>	<p>Standard clinical dose of DTG (most having an abacavir/lamivudine backbone)</p>	<p>(Bourgi <i>et al.</i>, 2020)</p>
	<p>Increased appetite</p>	<p>Interviews with clinicians who treat individuals on standard clinical dose ARVs and also surveys of individuals using ARVs (standard dose).</p>	<p>(Zakumumpa <i>et al.</i>, 2021)</p>
	<p>DTG caused increased clustering of large adipocytes, fibrosis, adipose enlargement (hypertrophy) and gene expression changes in both visceral fat and subcutaneous fat. DTG also increased ROS production.</p>	<p>Adipose stem cells were collected from healthy woman and treated with DTG (2 weeks with DTG (3.1 µg/mL)). Histology was done on SCAT and VAT of obese PLWH, and the primates were treated with similar plasma concentration to those of humans.</p>	<p>(Gorwood <i>et al.</i>, 2020)</p>
	<p>DTG interacts with melanocortin 4 receptor (MC4R), a receptor responsible for the modulating of leptin signalling in the central nervous system (Hill <i>et al.</i>, 2019). Mutations in MC4R are associated with heritable obesity (Adan <i>et al.</i>, 2006).</p>	<p>Comparative study of clinical trials and studies.</p>	<p>(Sax <i>et al.</i>, 2020)</p>

	A decrease in Adiponectin was associated with an increase in BMI.	50 mg, 96 weeks.	(Gatell <i>et al.</i> , 2017)
	None provided	50 mg of DTG per day	(Sculier <i>et al.</i> , 2018)
	The reduction in basal metabolic rate following suppression of plasma viremia, improved appetite due to lower inflammatory cytokine effects on the hypothalamus, and a reduction in the rate of protein turnover.	Individuals switched from a daily fixed dose of EFV/TDF/FTC to a daily fixed dose of DTG/ABC/3TC.	(Norwood <i>et al.</i> , 2018)
Hyperglycemia	None provided	Interviews with clinicians who treat individuals on standard clinical dose ARVs and also surveys of individuals using ARVs (standard dose).	Zakumumpa <i>et al.</i> , 2021)
	DTG inhibits the integration of the viral DNA by binding to the active site on magnesium (chelates magnesium). A decrease in magnesium can thus be a factor associated with DTG-induced insulin resistance.	All 3 cases reported: Switched to TDF/3TC/DTG (300 mg + 300 mg + 50 mg).	(Hirigo <i>et al.</i> , 2022)

	<p>Enlarged adipocyte size, independent of adiposity, is positively correlated with the development of insulin resistance and impaired metabolic health (Weyer <i>et al.</i>, 2000). DTG may damage adipose tissue, which explains the decrease in adiponectin and leptin. DTG causes oxidative stress, which is associated with insulin resistance.</p>	<p>Adipose stem cells were collected from healthy woman and treated with DTG (2 weeks with DTG (3.1 µg/mL)). Histology was done on SCAT and VAT of obese PLWH, and the primates were treated with similar plasma concentration to those of humans.</p>	<p>(Gorwood <i>et al.</i>, 2020)</p>
Hypertension	<p>Immuno-suppression associated with a low CD4 cell count leads to early vascular damage and subclinical atherosclerotic damage (Okello <i>et al.</i>, 2015). Participants without HIV viral suppression were at lower risk of developing hypertension compared with virally suppressed PWH.</p>	<p>Individuals who have been on ARVs for at least 2 years. No dosage stated.</p>	<p>(Musekwa <i>et al.</i>, 2021)</p>

From these reported side-effects, a potential dysregulation of adipose tissue is suggested. Given the known roles for chronic low-grade inflammation and increased oxidative stress in chronic conditions such as MetS and diabetes, in which obesity plays an aetiological role and which are commonly reported in HIV and generally after ARV use, it is warranted to investigate the effect of DTG on redox, which has not received much focus in the DTG literature. Furthermore, given the neurological side-effects of DTG and its known ability to cross the blood brain barrier (BBB), and since HIV-associated neurocognitive decline is thought to result from vascular dysfunction (including BBB disruption)(Shah *et al.*, 2016), it is important to consider whether DTG may affect vascular health. Furthermore, it has been suggested that high concentrations of ARVs in circulation also contribute to toxicity in the brain vasculature (Bertrand *et al.*, 2019), highlighting the importance assessing these changes in both the peripheral and central compartments.

Despite the side effects reported in Table 2.1, and the knowledge of the known effect of obesity on inflammation, redox status, and endothelial dysfunction, these potential sequelae have not been investigated sufficiently in the context of DTG. In the next sections, the potential mechanisms contributing to adverse redox and endothelial outcomes, with consideration of obesity will be reviewed.

2.3. Endothelial function and redox: inextricably linked

The vascular endothelium is a protective barrier of the arterial wall (Benjamin *et al.*, 2012). The endothelium plays a vital role in the control of vascular homeostasis. Additionally, it is implicated in the regulation of intracellular signalling, vascular tonus and permeability, the coagulation cascade and angiogenesis (Storch *et al.*, 2017).

The endothelial cells which form the vasculature are held together by complex structures consisting of numerous transmembrane proteins that interact both with binding ligands on adjacent cells and with associated intracellular partners. The two key junctional structures are a) tight junctions that incorporate members of the junctional adhesion molecule (JAM) family, EC-selective adhesion molecule and claudins, and b) adherens junctions that include proteins such as VE-Cadherin (Duong and Vestweber, 2020).

Claudin-5 is a tight junction protein mostly found in the endothelial cell layer of the brain, liver, kidney, and skin in humans (Greene *et al.*, 2019). Zona-occludin (ZO)-1 establishes a link between the claudins and occludin and the actin filament (Rao, 2008) as can be seen in Figure 2.2. It has been shown that decreased expression of ZO-1 is associated with severe plasma

leakage observed in multiple sclerosis (Kirk *et al.*, 2003) and diabetic rats (Hawkins *et al.*, 2007). VE-Cadherin is the most abundant protein present within the adherens junction. VE-cadherin is connected to the actin cytoskeleton via linker proteins β -catenin, α -catenin, and p120-catenin (Lagendijk *et al.*, 2014; Mitchell *et al.*, 2010) as seen in Figure 2.2. The actin filaments stabilise the tight junctions, thus their depolymerization leads to the disruption of tight junctions (Mitchell *et al.*, 2010). VE-cadherin appears to be conserved across species and zebrafish VE-cadherin has high homology with the VE-cadherin protein in humans (Mitchell *et al.*, 2010).

Research on the endothelium often incorporate animal models, including more recently, zebrafish (*Danio rerio*). The zebrafish endothelium and endothelial proteins are similar to those of humans. Van Leeuwen *et al.*, (2018) found that claudin 5a is the homologous gene in zebrafish equivalent to claudin 5 in humans. *In vitro* and *in vivo* studies demonstrate that the loss of claudin-5 results in increased motility of dorsal aorta endothelial cells and in a failure of the dorsal aorta to form a lumen (Yang *et al.*, 2020). Tight junction proteins such as ZO-1 are also found in zebrafish and more research is being performed on larvae and embryos (Schwayer *et al.*, 2019).

Most studies done on VE-cadherin in zebrafish are performed on larvae or *in vitro* models which mostly investigate the development of vasculature and the contribution and effect these tight- and adherens junctions have on it. A study done on zebrafish larvae showed that the knock down of VE-cadherin resulted in vascular developmental disruptions such as a disconnection in the blood flow between the heart and the periphery (Montero-Balaguer *et al.*, 2009).

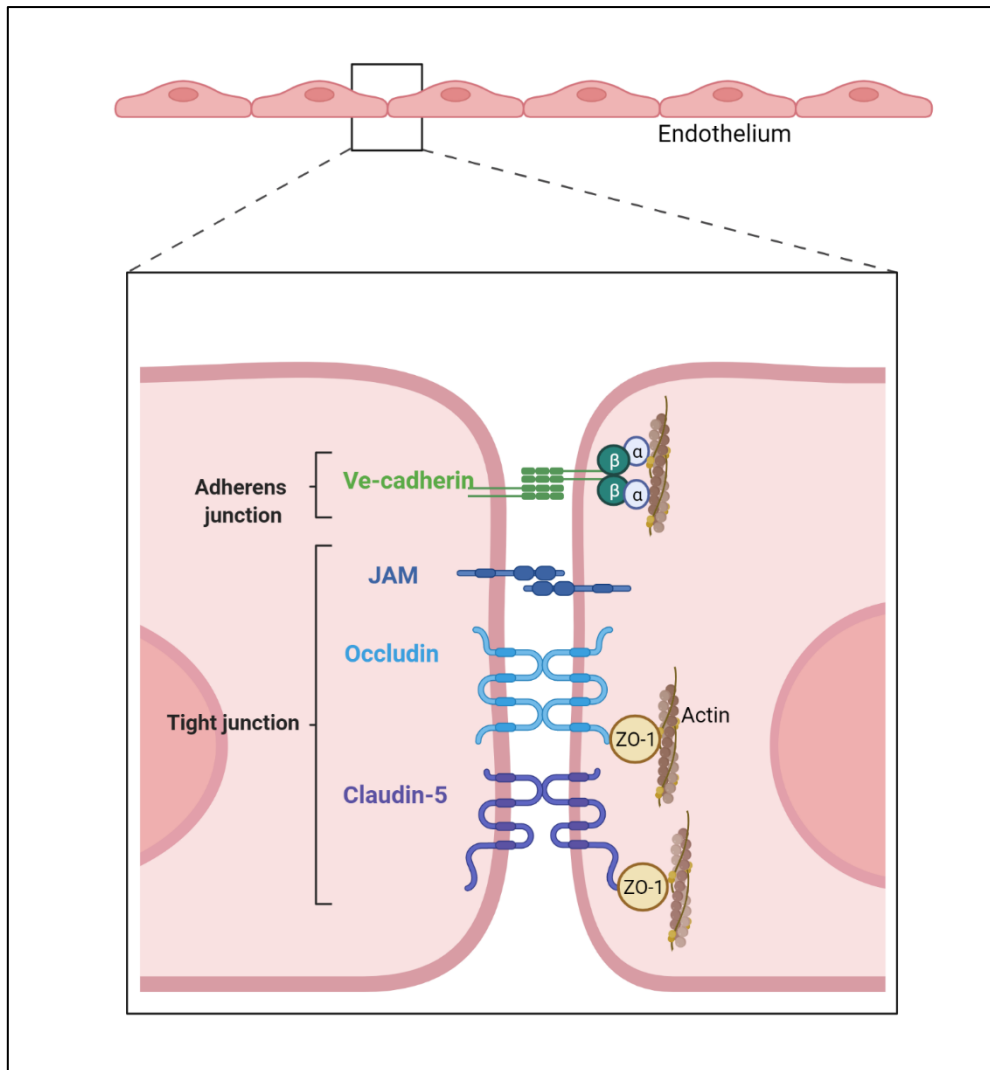


Figure 2.2: Tight junctions and adherens-junctions in the endothelium. VE-cadherin is linked to actin filaments via α - and β -catenin. Occludin and Claudin-5 is linked to the actin filaments via the interaction with ZO-1 (Biorender.com).

The vascular endothelium and the structures within are largely affected by inflammatory cells and their secretory products as described in Figure 2.3. Neutrophils – the main immune cell contributor to inflammation - are also able to release reactive oxygen species (ROS), proteases and cytokines, exacerbating the inflammatory response/milieu (Russo *et al.*, 2014) at the site of damage. Activated neutrophils (activated by pro-inflammatory cytokines etc. (Ronson, 1999), also produce superoxide via membrane-associated enzyme, nicotinamide adenine dinucleotide phosphate (NADPH) oxidase, which may also form hydrogen peroxide (H_2O_2). Myeloperoxidase, also released by neutrophils, is internalised by binding to the endothelial glycocalyx, prompting an increase in intracellular ROS formation (Granger *et al.*, 2010). Unquenched ROS increases the gap junctions between endothelial cells, thereby increasing the permeability of the blood vessel. Furthermore, ROS-associated endothelial

damage is known to promote clot formation and subsequent atherosclerosis. Furthermore, oxidized low density lipoprotein (Ox-LDL) (representing lipid peroxidation) accumulates in macrophages promoting the formation of foam cells, which lead to the development of an atheroma. Subsequently, overproduction of ROS facilitates the activation of cells that are involved in atherosclerosis and the formation and progression of lesion.

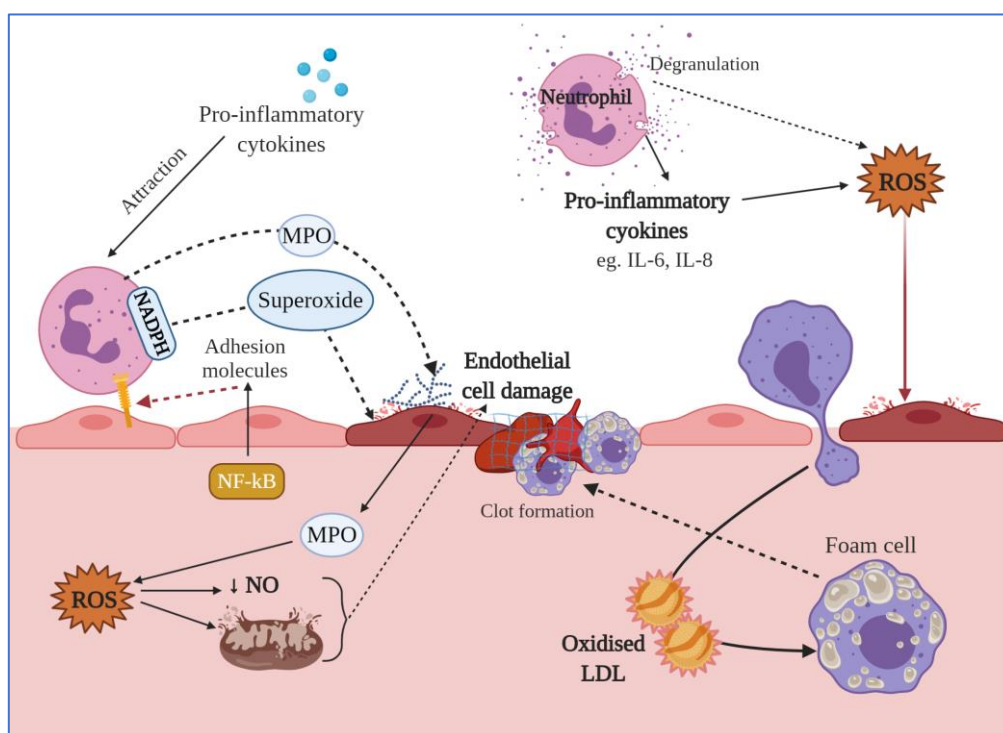


Figure 2.3: Inflammation and oxidative stress lead to endothelial damage through various mechanisms. Endothelial damage and lipid peroxidation are key risk factors for atherosclerosis. IL- Interleukin, MPO- Myeloperoxidase, NF-kB- nuclear factor-kB, NO- nitric oxide, LDL- low-density lipoprotein, ROS- reactive oxygen species, NADPH- nicotinamide adenine dinucleotide phosphate hydrogen, NO-nitric oxide.

Endothelial dysfunction is one of the main risk factors for diseases such as CVD and MetS (Jay Widmer and Lerman, 2014) and it is mainly characterized by the decrease in nitric oxide (NO). The reduced NO levels resulting from the excess ROS formation previously mentioned, results in relative vasoconstriction, an increase in endothelial adhesion molecules and decrease in cellular tight junction protein expression (Kovacs *et al.*, 2022). Under unhealthy circumstances, NO will bind to the superoxide radical, to decrease the availability of superoxide, but instead forms peroxynitrate, a toxic radical. Peroxynitrate is responsible for tissue damage and increased apoptosis (Ronson, 1999), but the chemistry behind these interactions are beyond the scope of this project. There are numerous adhesion molecules present, such as platelet endothelial cell adhesion molecule-1 (PECAM-1), CD99, CD47,

activated leukocyte cell adhesion molecule-1, and intercellular adhesion molecule-2 (ICAM-2), (Reglero-Real *et al.*, 2016). These molecules are released in response to stimuli of inflammatory cytokines, bacterial lipopolysaccharides (LPS) and ox-LDL. They promote cell to cell and/or cell to extracellular matrix adhesion, leading to, for example, foam cell accumulation on the endothelial cells, increased vessel wall thickness and subsequent obstruction and narrowing of vascular lumen.

In healthy circumstances vascular endothelial cell protein tyrosine phosphatase (VE-PTP) is associated with VE-cadherin and stays in a state of reduced phosphorylation at the endothelial junctions. Leukocyte adhesion to activated endothelial cells, through adhesion molecules, triggers the dissociation of VE-PTP from VE-cadherin, allowing phosphorylation of the latter (Broermann *et al.*, 2011). The phosphorylation of VE-cadherin through tyrosine 658 and 731 inhibits binding of p120 and β -catenin, leading to the decrease of VE-cadherin on the endothelial cell surface and endothelial permeability and transendothelial migration of leukocytes. Tumour necrosis factor- α (TNF- α) can also phosphorylate VE-cadherin and its catenins, contributing to the internalisation of VE-cadherin (Komarova *et al.*, 2017). It has been shown through an *in vitro* study that H₂O₂ rapidly increased tyrosine phosphorylation of the tight junction and adherens junction proteins leading to the dissociation of occludin from ZO-1, and E-cadherin from β -catenin (Rao *et al.*, 2002). It is also important to note that endothelial dysfunction in turn, also promotes pro-inflammatory and oxidative stress pathways via endothelial mitochondrial ROS driving vascular growth and remodelling (Cai and Harrison, 2000), leading to a vicious cycle of events.

The disassembly of tight and adherens junctions can lead to increased permeability and subsequent systemic inflammation. This is due to the transmigration of immune cells into the blood stream and into areas that do not require them. As seen in Figure 2.3. that this can have catastrophic outcomes. With the increased permeability, toxins can enter tissues from the blood stream. It can lead to a large variety of disease states, such as atherosclerosis, insulin resistance and a thrombotic state (Rajendran *et al.*, 2013).

Thus, in the context of DTG, it would be of importance to investigate effects not only on redox status, but also be able to link this to potential changes in expression of proteins indicative of vascular integrity, such as tight and adherens junction proteins.

2.3.1. Redox and endothelial dysregulation in the context of DTG and obesity

In the context of obesity, INSTIs (such as DTG) were illustrated to cause an increase in ROS production and mitochondrial dysfunction in proliferating adipose stem cells and to a lesser extent in adipocytes (Gorwood *et al.*, 2020). Mitochondrial ROS are traditionally seen as the

main source of intracellular ROS and, are therefore major mediators of ROS-induced damage (Rea *et al.*, 2018). DTG and EVG were shown to interfere with the respiration pathways in the mitochondria of CD4+ T cells (cultured from peripheral blood mononuclear cell) (Korencak *et al.*, 2019). Using oxygen consumption rate and extracellular acidification rate (which measures aerobic glycolysis by the acidity of the media) assays, DTG and EVG were shown to also increase mitochondrial ROS levels, confirming that they cause interference in the electron transport chain during oxidative phosphorylation. The ARV pre-treatment of multifunctional CD4+ T cells from HIV-negative, healthy individuals, demonstrated that both DTG and EVG caused a decrease in the overall immune response.

As an increase in adiposity and body mass lead to increased ROS, it is unclear whether or not the increased oxidative stress associated with DTG is as a result of the increased adiposity or the effects of the drug itself or even an interaction between the two factors. Of interest, there is still controversy regarding the weight gain reported after DTG treatment: while one group interprets this as an unhealthy weight gain that increases risk for co-morbidities, another group interprets the weight gain as a “return to health” (Kumar and Samaras, 2018). Answering this question will provide context for the data currently generated in obesity and *in vitro* models. Given this conundrum, the best approach would probably be to investigate effects of DTG in both lean and obese models in parallel.

The studies that have been done on the weight gain caused by DTG do not clearly state where this weight gain is. The location of the adipose accumulation determines if its healthy or unhealthy metabolic obesity (or overweight). More information on this topic will be explained in a later section. There is also not a standard percentage set to indicate significant weight gain (Hill *et al.*, 2019) which can lead to discrepancies when comparing the results of different studies.

Of course, it is near impossible to separate detrimental effects of vascular endothelium from changes in redox. For example, Letendre *et al.*, (2014) reported a direct DTG-associated increase in oxidative stress in the neuronal region by assessing the concentration of DTG in cerebrospinal fluid. This finding was also confirmed in a more recent study employing nano-formulated DTG administration in rats (Montenegro-Burke *et al.*, 2019b). Increased levels of H₂O₂ - an intermediate in the NADPH oxidase pathway and common biomarker for ROS levels - has also been shown to be involved in the rearrangement of the actin cytoskeleton, which is a potential mechanism by which it achieves disruption of the tight junctions. Additionally, increased levels of cytokines and growth factors have been shown to increase tyrosine phosphorylation of VE-Cadherin, which increases endothelial permeability and migration in cultured endothelial cells (Nwariaku *et al.*, 2004).

Hypertension, hyperglycemia and hyperlipidemia are all side effects of DTG (Kolakowska *et al.*, 2019). These factors are all closely associated with each other by oxidative stress, inflammation and or endothelial dysfunction. Figure 2.4 indicates how these side effects and the increase in oxidative stress and inflammation (and subsequent increase in proinflammatory cytokine levels), as mentioned above, affect the assembly and disassembly of tight junction and adherens junction proteins.

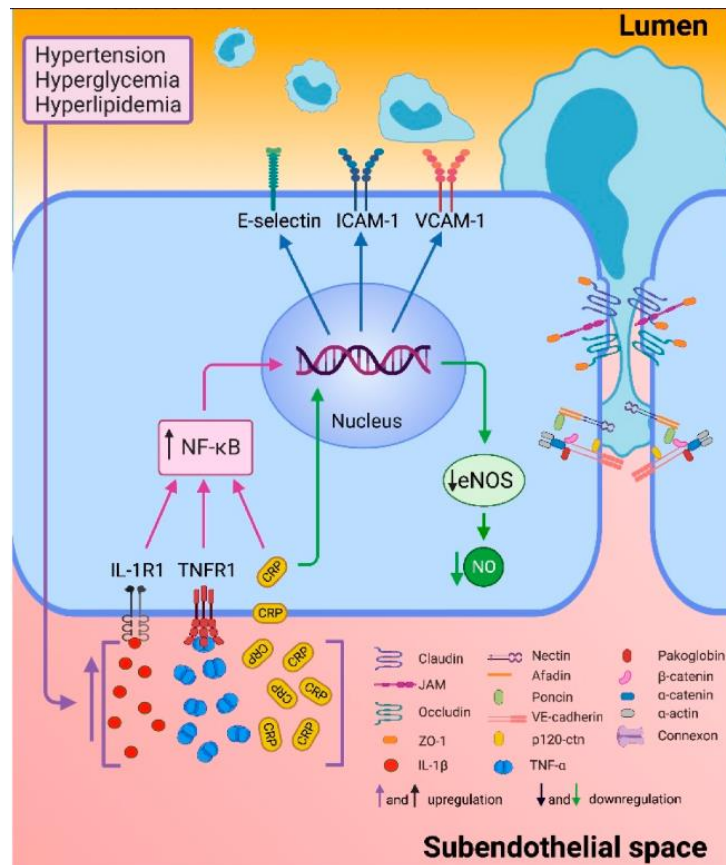


Figure 2.4: The effect of pro-inflammatory cytokines and adhesion molecules on the assembly and disassembly of the tight- and adherens junctions in the endothelial cells. Additionally, the transmigration of leukocytes is also depicted (from, Medina-Leyte *et al.*, 2021).

In addition, drug-interaction effects may further exacerbate the detrimental effects associated with DTG. In an *in vitro* study on human cell-lines (brain microvascular endothelial cells that constitute the BBB), the effect of DTG, sertraline and a combination of both on tight junction proteins in the BBB, showed that DTG (25 μ M which translates to roughly 10.5 μ g/mL of DTG) on its own was capable of decreasing the expression of ZO-1, Claudin-5 & JAM-2 genes, and in combination with sertraline (55 ng/ml) this was exacerbated, leading to further decreased tight junction expression (Cottrell *et al.*, 2013; Ma *et al.*, 2020). This suggests that DTG is

capable of decreasing the tight junction protein expressions, which would lead to loss of vascular integrity. DTG was also shown to increase the levels of TNF- α in these cells. The author of this paper concluded that the penetration of DTG into the BBB leads to neurotoxicity, microglial activation and neuronal apoptosis (Ma *et al.*, 2020). It has been shown that sertraline has been suggested to improve endothelial barrier dysfunction which is associated with depression (Pizzi *et al.*, 2009). Furthermore, since depression is a reported co-morbid outcome of DTG-use in HIV – for which the selective serotonin reuptake inhibitor sertraline may be prescribed – these data suggest a potential confounding effect in DTG users with depression, on endothelial membrane integrity. A suggested sertraline and DTG drug-drug interaction at the BBB may be the cause of reduced integrity of the former (Ma *et al.*, 2020). This warrants a more comprehensive investigation of the effect of DTG on tight junction proteins in other compartments.

Contradicting the above-mentioned reports, another study showed that human primary coronary artery endothelial cells treated with DTG (3.7 $\mu\text{g}/\text{mL}$) showed no effect on endothelial function or oxidative stress levels. Additionally, DTG decreased nuclear factor kappa B (NF- κB) indicating an anti-inflammatory effect. The authors suggested that DTG causes an anti-inflammatory effect through its ability to increase SIRT1, which is upstream of NF- κB , and which limits the transcription of the gene (Afonso *et al.*, 2017). The 3.7 $\mu\text{g}/\text{mL}$ of DTG is the equivalent dose to the 50 mg prescribed to humans. The decrease in cytokine levels were confirmed by another study, also indicating that DTG causes a decrease in IL-6 and an increase in NO levels. NO is associated with insulin sensitivity and endothelial function (Auclair *et al.*, 2020), as already mentioned. This study also used the dose of 3.7 $\mu\text{g}/\text{mL}$ of DTG on the same cell type. However, a study mentioned in Table 2.1. (Gorwood *et al.*, 2020) showed that adipose stem cells (ASCs) derived from healthy individuals which were then exposed to a DTG concentration of 3.1 $\mu\text{g}/\text{mL}$ for 2 weeks showed increased fibrosis, increased mitochondrial ROS and mitochondrial dysfunction (shown by increased mitochondrial mass and a decrease in membrane potential). This dose is similar to the dose given by the above mentioned study of Afonso *et al.*, (2017), however different outcomes were seen. Another meta-analysis done on randomized clinical trials (Hill *et al.*, 2018) which included all studies done on DTG containing regimens with a normal dose of 50 mg, showed that there was no increased risk for cardiovascular dysfunction.

This discrepancy in dosage and effect warrants the use of an *in vivo* model treated with the equivalent to the human dose of DTG to ascertain these effects.

2.4. Significance of obesity as potential confounder

Obesity is a major health concern in the South African clinical setting, with the highest prevalence of obesity in the sub-Saharan region recorded in South Africa (Alaba & Chola, 2014). According to the latest WHO data (2016), more than 50% of South Africans (male and female) are overweight or obese (body mass index (BMI) ≥ 25).

Adipose tissue is a complex tissue consisting of multiple cell types, with both beneficial and potentially detrimental functions. Not all adipose tissue is equally detrimental to health. There are two types of adipose tissue, namely white adipose tissue (WAT) and brown adipose tissue (BAT). BAT is dense with mitochondria and functions primarily to generate heat. WAT is the most abundant tissue in the body and is responsible for the secretion of adipokines and adipocytokines (Corrêa *et al.*, 2019; Omran and Christian, 2020). WAT is associated with increased risk of developing MetS as most WAT is found in the abdominal/visceral area. This is supported by the metabolically healthy vs. metabolically unhealthy obesity (MHO vs MUO) phenomenon. The distribution and site of fat deposition plays a vital role, with increased abdominal or visceral fat deposition recognised as a greater risk factor for developing disease than subcutaneous accumulation of fat (typically in the hip or thigh region) (Cypess and Kahn, 2013; Gómez-Hernández *et al.*, 2016). Therefore, given the dispute regarding DTG-associated weight gain, it is perhaps important to first characterise the nature of weight gained in terms of site of fat deposition and the nature of fat deposits, to assess whether it represents a metabolically healthy phenomenon, or not.

The outcomes of the study done by Couturier *et al.*, (2018) showed that DTG accumulation was mostly in subcutaneous adipose stromal vascular fraction (SVF) and lymph nodes. In patient one, DTG was not detectable in visceral adipose SVF, but in subcutaneous SVF, lymph nodes and adipocytes. The latter was also the case for patients three to six. This may indicate that the weight gain or increase in adiposity associated with DTG are not necessarily considered metabolically unhealthy and this should be further investigated.

However, regardless of the outcome in this regard, it is important to consider that hyperglycemia is another commonly reported outcome associated with DTG administration. This suggests insulin resistance, which is mechanistically similar to obesity. Therefore, I briefly discuss adipose dysregulation in this context below.

2.4.1. Adipose dysregulation in obesity

On the one hand, adipose tissue is imperative in immunity - host defence, injury responses, as well as the acute production and secretion of inflammatory chemokines and cytokines are required for the execution of an acute response to stressors/stimuli threatening homeostasis (Makki et al., 2013a). Adipose tissue is also an endocrine and storage organ necessary for energy homeostasis. Not only does adipose tissue consist of adipocytes, but it also comprises of other cells (e.g., endothelial and immune cells, fibroblasts, and fibroblastic pre-adipocytes) that are capable of secreting hormones and cytokines (adipokines or adipocytokines). However, several molecules secreted and/or activated by adipose tissue (including adipokines) have the capacity to promote inflammation, activate an immune response (via macrophage recruitment etc.) and lead to a subsequent increase in ROS (Alam *et al.*, 2012; Andreicuț *et al.*, 2018) as previously discussed. The increased glucose metabolism and free fatty acid levels associated with obesity are directly linked to increased oxidative stress and inflammation. These factors are associated with the development of chronic inflammatory conditions such as diabetes and MetS, as well as CVD. These adverse signalling events in adipose tissue in obesity are summarised in Figure 2.5.

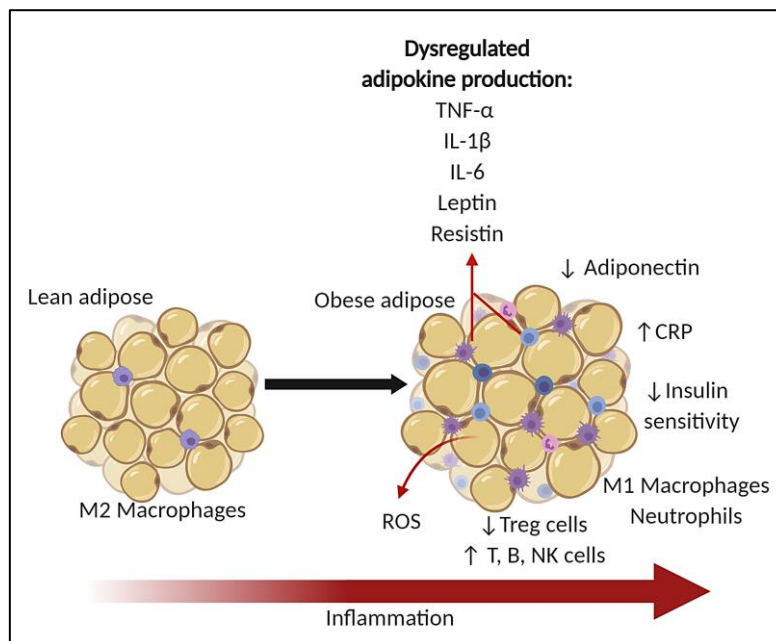


Figure 2.5: Adipose tissue undergoing an inflammatory maladaptive response in obesity (adapted from Makki et al., 2013).

In terms of specific mechanisms involved, oxidative stress and damage occurs when the increased ROS levels overwhelm the endogenous antioxidant capacity. In terms of ROS production, NADPH oxidase is a central role player. Furthermore, NADPH subunits are increased in adipose tissue and may therefore be one of the factors contributing to the increased oxidative stress associated with increased adiposity and associated chronic diseases (Figure 2.6; Matsuda and Shimomura, 2013). Immune cells associated with adipose tissue also contribute to the inflammation and oxidative stress associated with obesity. For example, as shown in Figure 2.5, in individuals with obesity there is greater infiltration of macrophages – in particular the M1, pro-inflammatory phenotype - in the adipose tissue which also produce ROS.

Another inflammatory component dysregulated due to obesity is the NOD-, LRR- and pyrin domain-containing protein 3 (NLRP3) inflammasome. Inflammasomes are cytoplasmic multi-protein complexes that recognise danger signals and cleave pro-inflammatory cytokines into active cytokines and form part of the innate immune system (Liu *et al.*, 2017). The NLRP3 inflammasome has been shown to impair adipose tissue sensitivity, suggesting a role in the development of MetS. NLRP3 activation by NF- κ B initiates a cascade of intracellular events, culminating in the cleavage of pro-interleukin 1 β (pro-IL-1 β) by caspase-1, to form active IL-1 β . Research done in mice shows that obesity triggers NLRP3 activation to increase the secretion of IL-1 β , subsequently resulting in insulin resistance (Rea *et al.*, 2018).

Furthermore, the antioxidant enzymes of adipose tissue (such as superoxide dismutase 1 and glutathione peroxidase) in individuals with obesity are decreased – suggesting a gradual depletion of antioxidant capacity in obesity. This results in ineffective quenching of the increased free radical levels (Furukawa *et al.*, 2004), thus increasing risk of oxidative damage to tissues such as the endothelium.

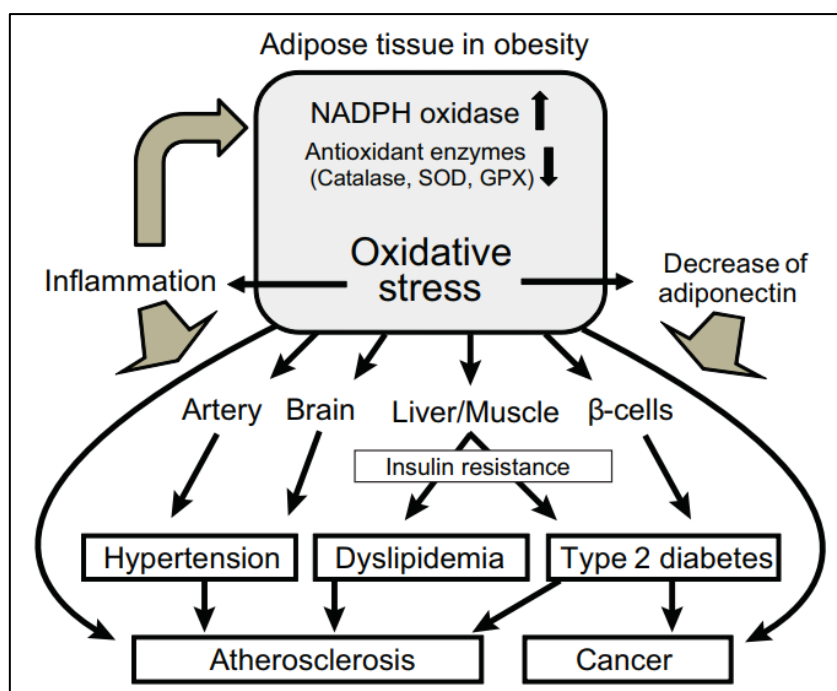


Figure 2.6: The effect of oxidative stress in adipose tissue on other physiological pathways which may lead to other disease states (from Matsuda and Shimomura, 2013).

Specifically relevant to the topic of this thesis, DTG is reported to better penetrate adipose tissue than other NRTIs (e.g., Tenofovir), suggesting that their effectiveness may be decreased by increased adiposity (Couturier *et al.*, 2018). This may be due to the hydrophobic nature of DTG. Indeed, it has also been shown that DTG exhibits long-term retention in fat cells (Couturier *et al.*, 2018) as DTG was found in cadavers from which tissue was only harvested several days after arrival. Therefore, DTG may have the potential to significantly alter signalling from adipose tissue in the context of inflammation and oxidative stress, which may then have an impact on endothelial health and CVD risk. Obesity may exacerbate the inflammatory outcome in HIV, as well as affecting bioavailability of sequestered ARV drugs.

2.5. Methodological considerations

2.5.1. Inclusion of both sexes

Peripheral obesity, characterized by an accumulation of subcutaneous adipose tissue, is more prevalent in woman. As previously discussed, the accumulation of subcutaneous fat is less concerning than the accumulation of visceral fat and thus less associated with related pathologies (Snijder *et al.*, 2003). However, central or abdominal obesity is more common in

men and consists of an accumulation of visceral adipose tissue (Gómez-Hernández *et al.*, 2016).

DTG is administered to any individual with HIV, irrespective of their weight. When an individual is obese pre-treatment, this might affect the efficacy of the drug and may have other or exacerbated adverse effects. In the randomized ADVANCE study, the weight gain associated with the use of DTG was higher in females than in males (Bakal *et al.*, 2018; Sax *et al.*, 2020; Venter *et al.*, 2019), emphasizing the inclusion of both sexes in this study.

Furthermore, Burek *et al.*, (2010) showed in an *in vitro* study done on murine heart and brain endothelial cells that estrogen has an effect on claudin-5 levels. Estrogen upregulated the expression of claudin-5 more than two-fold, and it also increased VE-cadherin slightly. Although the mechanism of this phenomenon is more intricate, it proves that both sexes should be included in a study, as different hormones, found in different concentrations in males and females can affect the results.

2.5.2. Choice of animal models

2.5.2.1. Consideration of rats in research

Rats have been used in research for many decades. They have been used to simulate various diseases, such as diabetes, obesity and CVD. Rats have been used to study CVD and atherosclerosis (Jia *et al.*, 2020; Xiangdong *et al.*, 2011) and methodology for calculating human equivalent treatment doses using body surface area and metabolic rate adjustments are well described (Nair and Jacob, 2016; Reagan-Shaw *et al.*, 2008). Additionally, rats have been used in studies which investigate the vasculature (especially in their aorta) (Rameshrad *et al.*, 2016). Rats will therefore be an excellent model in which to assess tight junction integrity in response to DTG.

Since housing and maintenance of rats are costly, especially in a long duration protocol, the decision was made to assess potential confounding effects of obesity in a parallel study in adult zebrafish for consideration in future studies.

2.5.2.2. Consideration of zebrafish in research

The Zebrafish (*Danio Rerio*) has become an increasingly popular model for research due to certain genetic similarities to humans. Zebrafish are easy to house and breed and their behaviour is easily observable and quantifiable. Additionally, they have been increasingly

used to study metabolic disease states, such as obesity and other related metabolic conditions (Faillaci *et al.*, 2018), with diabetes and hyperglycemia being two examples (Ghaddar, 2020). The first diet-induced obesity model in zebrafish was established by Oka *et al.*, in 2010. The adult zebrafish size makes it easier to visualise individual organs in response to disease/treatment interventions when compared to the larval model.

There is a relative lack of data in zebrafish models in the niche of ARV and endothelial health, despite its unique suitability for different aspects, especially microscopic visualisation. By employing this model in addition to the rat model, the robustness of results obtained can be validated comparatively across the two models. The zebrafish model will add more information to this topic which is not necessarily accessible through the use of rodent models, such as the obesity component.

In adult zebrafish, the major arteries are the ventral aorta and the dorsal aorta. Oxygenated blood from the gills are sent to efferent branchial arteries, which merge, forming the dorsal aorta (Hu *et al.*, 2001) The vascular wall of zebrafish has similar vessel organization as in other vertebrates (Hoareau *et al.*, 2022) They are usually structured in three layers: the tunica intima, media and adventitia or externa, from lumen to periphery. These layers are more evident in large vessels and are not found in capillaries and venules. The intima is composed of endothelial cells and a layer of extracellular matrix that forms a basement membrane (Hoareau *et al.*, 2022). Miano *et al.*, (2006) was the first study done on the development of the dorsal aorta from 7dpf to 3 months post fertilisation (mpf) (Figure 2.7). They have shown that in addition to endothelial cells, the dorsal aorta also contains vascular smooth muscle cells.

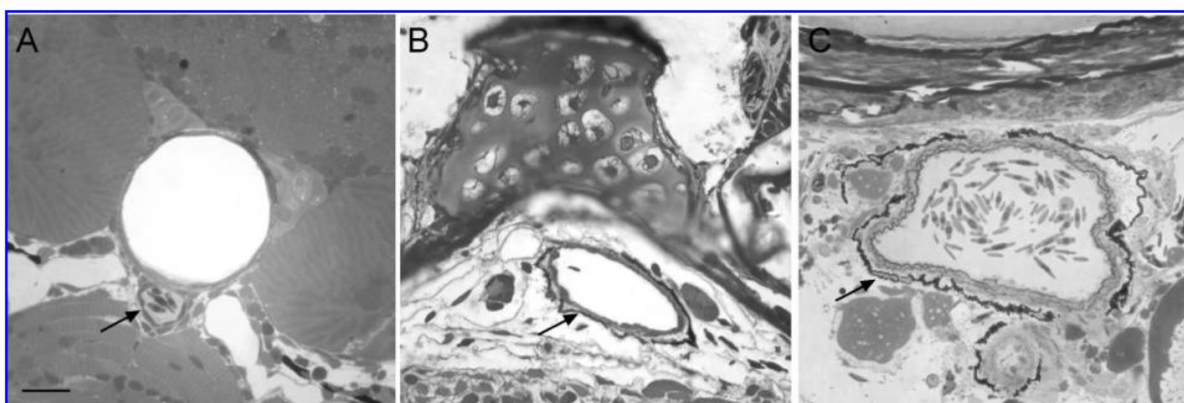


Figure 2.7: The development of the dorsal aorta from A) 7dpf to B) 1mpf and C) 3-month-old adult zebrafish. The aorta is depicted by the black arrow. From: (Miano *et al.*, 2006).

Thus, given this similar vascular physiology, zebrafish are a good model for investigation of both central and peripheral effects of DTG. Furthermore, the zebrafish tight junction molecules are mostly conserved and would serve as an excellent model for imaging the change in tight junction expression caused by the effects of DTG.

2.5.3. Inducing obesity in zebrafish

Zebrafish have recently been used to study and model metabolic disease, as they possess metabolic organs, such as digestive organs, skeletal muscle and adipose tissue similar to that of humans (Faillaci *et al.*, 2018; Zang *et al.*, 2018). They have the conservation of specific metabolic pathways that are involved in energy homeostasis, cholesterol and lipid metabolism, and adipocyte differentiation and the formation of adipose (Zang *et al.*, 2018). Additionally, in zebrafish, lipids are also stored in intramuscular, visceral and subcutaneous adipocytes (Song and Cone, 2007). It is clear that the zebrafish pose an appropriate model for the investigation of metabolic disruptions/dysregulation and to understand and investigate some factors associated with obesity.

However, this model is not without limitations. Zebrafish do not possess brown adipose tissue (Zang *et al.*, 2018) and zebrafish leptin protein is only 19% identical to human protein (Michel *et al.*, 2016). Of further relevance, leptin and the leptin receptor are not expressed in adipose tissue in zebrafish, but in the liver. However, transgenic zebrafish deficient in the leptin receptor exhibits interrupted glucose homeostasis (Michel *et al.*, 2016; Myers *et al.*, 2010) also indicating that there is no role of leptin in adipostasis in zebrafish. Thus, as in rodents, zebrafish models may be useful tools, as long as users are aware of species differences in the systems to be investigated.

In the context of inducing obesity, and perhaps due to their somewhat different leptin physiology, zebrafish can be more easily made obese by simple overfeeding, when compared to rodent models, where specific high sugar or high fat diets are required, which come with their own downstream health complications. The first diet-induced obesity study in zebrafish (Oka *et al.*, 2010) employed overfeeding of adult zebrafish with high fat freshly hatched *Artemia* shrimp. Another study reported inducing obesity by simply overfeeding fish on commercially available fish food (Zang *et al.*, 2017). A comparison between zebrafish fed a high-fat diet (HFD) or a normal-fat diet (NFD) showed that both dietary regimens can induce a significant increase in body mass (Faillaci *et al.*, 2018). In the current context, where the desire is not to induce MUO characteristic of a Western lifestyle, but rather simply increased adiposity, overfeeding without the increased fat component is in our opinion the best choice, as a high fat diet may prevent detection of DTG-induced effects.

2.6. Rationale

DTG is an integrase inhibitor, now being used as a first line treatment in a combination with abacavir and lamivudine. DTG has been associated with a wide variety of side effects. However, the research done on these side effects are contradictory in terms of weight gain (is it metabolically unhealthy or healthy weight gain and what percentage of weight gain is seen as significant), monotherapy vs combination therapy of DTG and the dosages used in research are not standardised and the results thereof vary.

This warrants the use of *in vivo* models to establish what the effect of DTG monotherapy, without the confounding effect of the HIV, with a dose as close to the human dose, is on endothelial dysfunction, as endothelial dysfunction is associated with obesity and CVD. The use of an obese model will also clear up some controversies around the weight gain and adipose harbouring effects of DTG.

2.7. Hypothesis statement

After the review of literature, it is evident that endothelial dysfunction is a common denominator in the side effects of ARV use and HIV.

We hypothesised that chronic Dolutegravir treatment will have adverse effects on redox status and vascular endothelial health, specifically in terms of tight junction protein expression. We furthermore hypothesized that obesity would exacerbate these effects.

AIM

We aimed to investigate whether or not Dolutegravir causes oxidative stress and endothelial dysfunction. Furthermore, we aimed to determine the association between oxidative stress status and measures of endothelial dysfunction in this context, with consideration of obesity as potential confounder.

OBJECTIVES

In order to address our aims, two parallel animal models were employed. Specific objectives for each model are listed below.

Part 1 – Zebrafish model

1. To induce obesity in adult zebrafish using an overfeeding protocol.
2. To administer dolutegravir chronically.
3. To assess tight junction protein and adhesion molecule expression in peripheral and central vascular endothelium.
4. To assess the ROS levels in the liver as a measure of oxidative stress and damage.

Part 2 – Rodent model

1. To execute a chronic dolutegravir intervention study in healthy male and female Wistar rats
2. To determine the effect of dolutegravir on body mass and organ mass.
3. To assess tight junction protein and adhesion molecule expression in peripheral and central vascular endothelium.
4. To assess the redox profile of the endothelium in the liver of the rats as a measure of oxidative stress and damage.

CHAPTER 3

3. MATERIALS AND METHODS

Experiments were conducted in two main experimental models, namely adult zebrafish and rodents (Wistar rats). Similar analysis was performed on samples generated in the different models and will be described after descriptions of model-specific procedures.

3.1. Dolutegravir exposure in lean and overfed adult Zebrafish

3.1.1 Ethical considerations

All protocols on adult zebrafish were ethically cleared by the Stellenbosch University Animal Research Ethics Committee (ref# ACU-2019-21999). The health and well-being of each fish was monitored daily using monitoring sheets, checked by SAVC-registered staff members.

3.1.2 Experimental groups and procedures

Four-month-old wildtype zebrafish (24 male and 24 female) were obtained from the Zebrafish Research Unit in the Division Clinical Pharmacology. Zebrafish were randomly split into four sex-matched groups (n=12 per group; n=6 males and n=6 females per group): control, overfed, lean DTG and overfed DTG.

3.1.3 Overfeeding protocol

The control group was fed twice a day (8am and 6pm) with dry semi-floating micro pellets (Hikari), at a total daily dose equating to 3% body mass (12.13 mg/fish/day). The duration of the overfeeding protocol was 4 weeks. The constituents of the pellets are described in Appendix C. The overfed group was fed six times a day with dry Hikari pellets (36.41 mg/fish/day). These feeding procedures are summarised in Figure 3.1. The overfeeding protocol was adapted from literature (Ghaddar *et al.*, 2020; Oka *et al.*, 2010; Zang *et al.*, 2017), with the weight of the food adjusted to the weights of the zebrafish in our laboratory. At all feedings, zebrafish consumed all the food within 10 minutes.

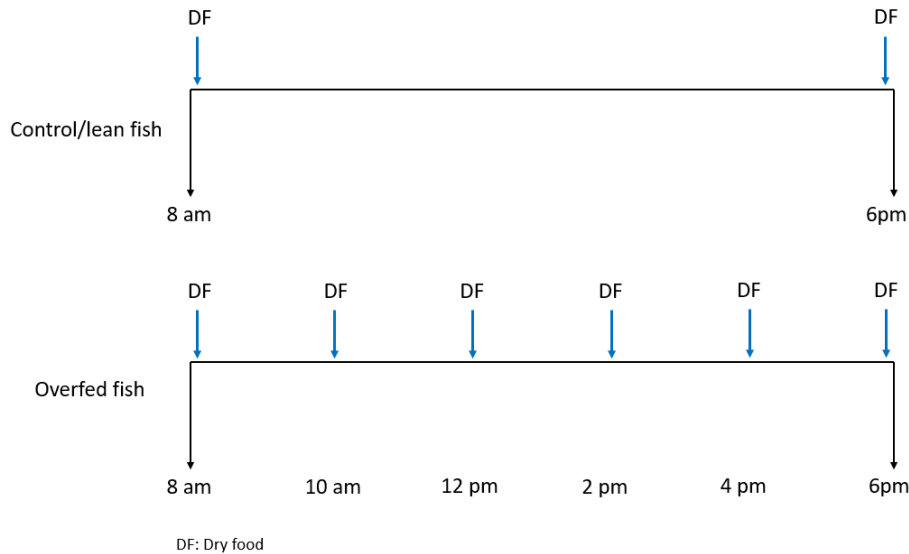


Figure 3.1: The overfeeding protocol used in the study. DF- Dry food.

3.1.4 Dolutegravir administration

DTG was extracted from Olegra (50 mg) tablets using liquid-liquid extraction and purity confirmed using high-performance liquid chromatography. This procedure formed part of the MSc thesis of another student (N Henning, MSc 2022).

DTG was administered for 2 weeks (the last 2 weeks of the overfeeding 4-week protocol). The protocol followed is summarised in Figure 3.2. In order to derive a zebrafish dose equivalent to the 50 mg/day DTG administered in humans, a dose conversion calculation was performed incorporating body surface area, as well as the human:ZF Km ratio to account for differences in metabolic rate, as shown in Table 3.1.

Human dose = Animal dose $\times \frac{\text{Animal } km}{\text{Human } km}$ (Nair and Jacob, 2016; Reagan-Shaw *et al.*, 2008),

where *km* is the correction factor (Km) is estimated by dividing the average body weight (kg) of species to its body surface area (m²) (Nair and Jacob, 2016).

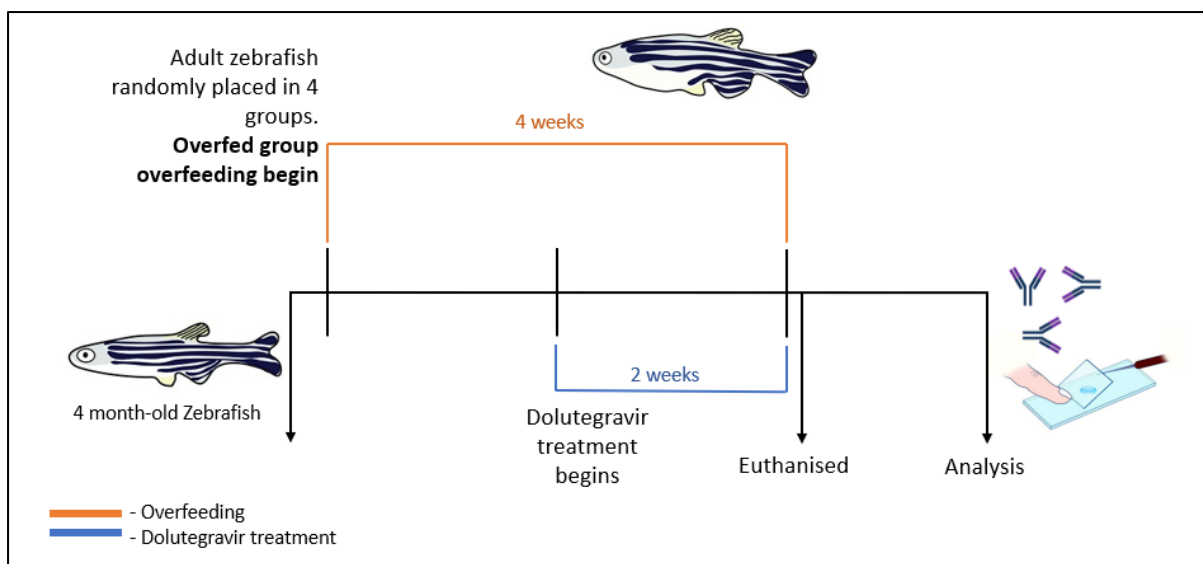


Figure 3.2: Timeline of the adult zebrafish study.

Table 3.1: The values used to calculate the doses given to an individual adult zebrafish and rat, which is equivalent to the human dose

	Humans	Adult zebrafish	Rats
Body surface area (m ²)	1.73 ^A	6.4x10 ⁻⁴	0.03566 ^C
Average body mass (kg)	70 ^B	4.045x10 ⁻⁴	0.2192 ^C
Km	40.462	0.632	6.147
Dose (mg/kg)	0.714	45.754	4.7
Dose (mg)	50	0.0185	1.03
A-(Pai, 2012), B-(U.S Department of Health and Human Services <i>et al.</i> , 2019), C-(Gouma <i>et al.</i> , 2012).			

3.1.4.1. Coating of fish pellets with DTG

According to the Food and Drug Administration (FDA) (Reference ID: 3310563, 2017) 0.076 mg of DTG is soluble in 1 mL of ethanol (EtOH). One mg of DTG was dissolved in 13.16 mL EtOH for the stock solution. The stock solution was vortexed for at least 1 minute to make sure that the DTG was dissolved. 2.92 mL (which contains 222.115 µg of DTG (18.5 ug x 12 fish per tank)) of the stock was taken out and placed on 73 mg (6 mg x 12) of pellets. Test tubes

were then placed in the MiVac (Genevac miVAC duo sample concentrator) for at least 45 minutes to evaporate the EtOH. DTG is highly non-polar and highly protein bound (Min *et al.*, 2011) and will therefore preferentially bind to the high protein fish pellets, rather than to the EtOH, thus leaving the DTG behind on the pellets. This procedure is summarised in Figure 3.3.

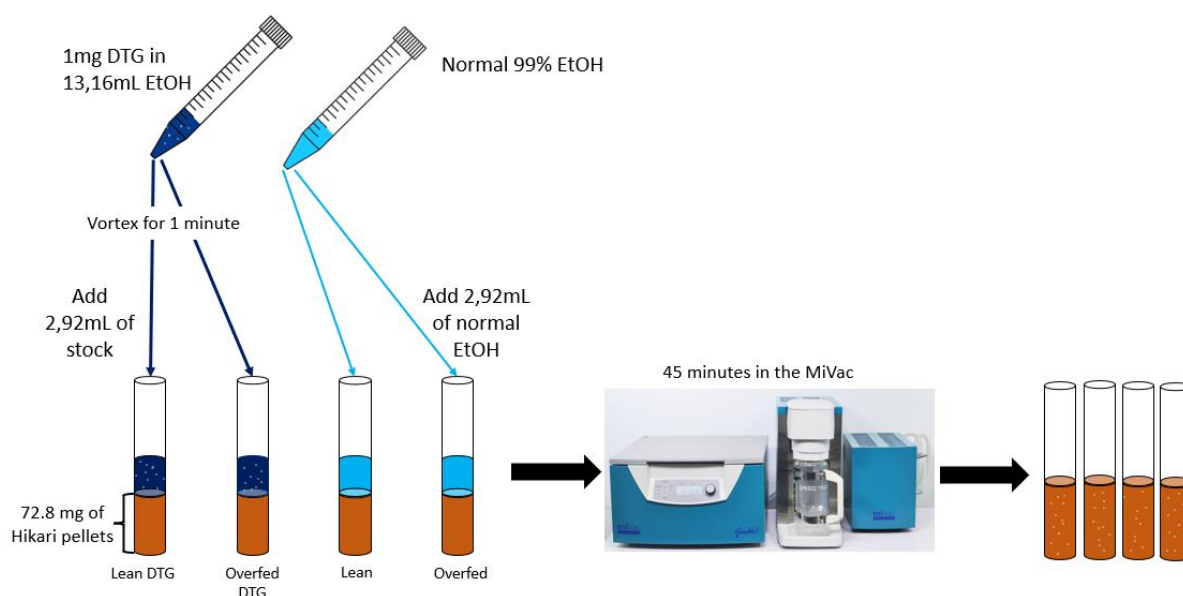


Figure 3.3: The coating of the Hikari fish pellets with DTG.

3.1.5 Sample collection

Adult zebrafish were euthanised by means of tricaine overdose (0.04 mg/mL) by immersion. Body mass was determined for each fish before dissection. Half of each group (n=6) was utilised as intact tissue slices for histology and immunofluorescence; the other half was used for the dissection of the livers. For histology samples, zebrafish heads were cut behind the gills (Figure 3.4.), whereafter the head and body sections were mounted separately in tissue freezing media (OCT; 14020208926, Leica) and frozen in liquid nitrogen-cooled isopentane. Zebrafish heads and bodies were stored at -80°C until sectioning and fluorescence staining of the samples. Livers were harvested and snap frozen in liquid nitrogen, before being stored at -80°C until analysed using a commercial H₂O₂ assay.

It is important to note that ethical consideration was taken and the repeated netting could cause the fish increased stress which could have potential confounding effects to this study. For this reason, fish were not separated into male and female groups, as the fish were harvested and prepared as they were caught to ensure less stress. In the future, it will be

better to separate the males and females into different tanks the night before euthanasia, to ensure equal amounts of males and females used for histology and liver extraction.



Figure 3.4: The figure of how the body of zebrafish were harvested. The red arrow indicates the direction of sectioning for the dorsal aorta. The black arrow indicates the direction of sectioning for the brain and bulbous arteriosus.

3.2. DTG exposure in rodent model

3.2.1. Ethical considerations

All protocols on Wistar rats were ethically cleared by the Stellenbosch University Animal Research Ethics Committee (ACU-2021-22035). Care was taken to minimise the number of animals used whilst still allowing for sufficient statistical power. All experiments on animals were carried out in accordance with the guidelines of the South African National Standard (SANS).

3.2.2. Experimental animals

Young (8-week-old), Wistar rats (total=24, male n=12, female n=12) were obtained from the Stellenbosch University Faculty of Medicine and Health Sciences Animal Facility. Rats were divided into 2 groups: control (placebo-treated, 6 males and 6 females) and DTG-treated (6 males and 6 females). Rats had access to standard rat chow (Imbani Nutrition, Western Cape, South Africa) and tap water *ad libitum* while being exposed to a 12hr light/dark cycle (lights on at 5:30 a.m.). The temperature in the housing facility was controlled at 21°C. Rats were housed as 3 rats per cage in compliance with husbandry guidelines, with males and females housed

in separate cages. For enrichment, a small section of PVC piping was placed in the cage, through which the animals could walk and in which they could sleep.

Rats were handled daily and during weighing in order to ensure that they were accustomed to the people working with them and were less stressed when handling was necessary for euthanasia. All rats were fed jelly blocks for a week during the acclimatization period, to accustom them to the process of administration of the treatment in jelly blocks.

Rats were monitored daily. Their food and water supply were checked every day and topped up when needed. The daily monitoring sheets were filled in daily to ensure that the health and well-being of each rat was taken care of. Rats were weighed Mondays and Thursdays to keep track of the weight of the rats over the period of the study.

3.2.3. Intervention: Dolutegravir administration

Young (8-week-old) Wistar rats were entered into the treatment protocol and treated with DTG (1.03 mg/day) administered in jelly blocks, once daily for 12 weeks. The same DTG that was extracted for the zebrafish study was used for this study. This dosage was determined using the same procedure (Reagan-Shaw *et al.*, 2008) explained in detail in table 3.1. Control rats also received jelly blocks without any treatment additions to eliminate any potential confounding effects of the jelly itself. The jelly was placed in a silicone cube tray (750 μ L), whereafter the DTG was placed on top of the jelly (at room temperature) and then covered with the remaining jelly (250 μ L) to ensure that the DTG was in the middle of the jelly block. The jelly was left to set at 4°C for at least 2 hours.

3.2.4. Sample collection

After 12 weeks of treatment, the rats were euthanised by sodium pentobarbital overdose (Eutha-Naze, 83/91, Bayer) (200 mg/kg body mass). A portion (\pm 2 cm) of the descending aortas and the middle hemisphere of the brain (Figure 3.5.) were harvested, mounted in tissue freezing media (OCT; 14020208926, Leica) and frozen in liquid nitrogen-cooled isopentane, before storage at -80°C until batch analysis for sectioning and fluorescence staining. The livers were harvested, weighed, cut into smaller sections and the lowest part of the left lobe was snap frozen in liquid nitrogen. Tissues were stored at -80°C and protected from light until further processing for determination of ROS content.

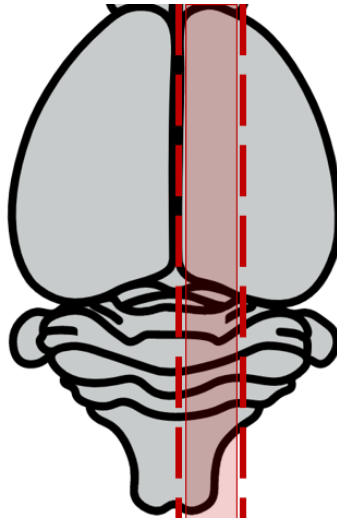


Figure 3.5: The rat brain section used for this study (indicated by the red section). The left and right lobes were separated, and the right lobe was again cut in half, where this study used the innermost part of the brain.

3.3. Sample analysis

3.3.1 Reactive oxygen species (ROS)

H₂O₂ levels were assessed as a representative indicator of reactive oxygen species present in the livers of rodents and adult zebrafish using a hydrogen peroxide kit, (ElabScience #E-BC-K102-S) according to manufacturer's protocol, with some minor modifications. In a 96-well plate, 100 µL of Reagent 1 was incubated at 37°C for 10 minutes whereafter 10 µL supernatant and 100 µL of reagent 2 was added. Supernatants of the different models were prepared as follows: Adult zebrafish livers were pooled in groups of two in order to get 10 mg liver tissues in 1 mL phosphate buffered saline (PBS) (P4417-100TAB, Sigma-Aldrich; Germany) and 10 mg of rat liver was placed in 1 mL cold PBS for homogenisation. The livers were homogenised (Bead Ruptor Elite, OMNI International) (6.95 m/s, 4 cycles of 15 seconds each, separated by 1 minute) and centrifuged (10000 xg for 10 minutes) whereafter the supernatant were frozen at -80 °C until analysis.

Bradford protein detection: Protein concentrations were determined to correlate H₂O₂ to protein concentrations in each sample. Bradford assay (Bradford, 1976.) was performed following the standard laboratory protocol.

3.3.2. Histology and tight junction protein expression of the rat and zebrafish aorta

Frozen rat aorta and zebrafish bodies were sectioned at 6 μm and 10 μm respectively, at -35°C, using a Cryostat (Leica, Germany). Sections were stained with haematoxylin and eosin (H&E) stains for morphology and immunofluorescent staining was performed for VE-cadherin, Claudin 5 and ZO-1 (proteins forming tight and adherens junctions) as described below.

3.3.2.1. H&E protocol and image analysis

Rat aorta and brain, and adult zebrafish dorsal aorta, bulbus arteriosus and brain was stained with H&E following standard laboratory protocol. H&E sections were visualised at using a light microscope (Eclipse, E_i, Nikon).

3.3.2.2. Fluorescence staining protocol and image analysis

Tissues were freshly sectioned and allowed to thaw at room temperature for 30 minutes (not frozen before sectioning). Wax circles (Z377821-1EA, Advanced PAP PEN, Sigma, Japan) were drawn around tissue sections. Sections were fixed in 4% paraformaldehyde (158127, Sigma-Aldrich, USA) for 15 minutes. Sections were washed three times with PBS for 5 minutes each. Sections were blocked for 90 minutes with 5X blocking buffer (BB): 20% fetal bovine serum (FBS) (Biowest, S181Y-500), 5% Donkey serum (S217G, Celtic Diagnostics, South Africa), 75% PBS-T (PBS +0.1% Tween 20) (Tween: P-1379; Sigma; Germany) for permeabilization. The sections were incubated with primary antibodies (Table 3.2.) in 1X blocking buffer overnight in 4°C. Sections were washed three times in PBS for 5 minutes each. Secondary antibodies (Table 3.2) were added in 1X BB and incubated for 2 hours at room temperature. Sections were washed three times in PBS for 5 minutes each. Slides were mounted using fluorescence mounting media (S3023 Dako Mounting Media, Diagnostech). Fluorescently stained tissue sections were visualized using an inverted microscope (Nikon Eclipse Ti2) using the provided software (NIS-Elements D 5.30.02 64-bit.Ink). Mean fluorescent intensity were measured by using ImageJ, as demonstrated in Figure 3.6.

Table 3.2: Antibodies used for rat descending aorta and adult zebrafish dorsal aorta staining.

Antibody	Source (Catalogue number)	Dilution
VE-cadherin (Goat)	R&D Systems, USA (AF938)	1:50
Claudin-5 (Rabbit)	Novus Bio, USA (#NBP2-66783)	1:100
ZO-1 (Mouse)	Invitrogen, USA (#33-9100)	1:100

Alexa fluor donkey anti-goat 350	Invitrogen, USA (A21081)	1:250
Alexa fluor donkey anti-rabbit 555	Invitrogen, USA (A31572)	1:500
Alexa fluor donkey anti-mouse 388	Invitrogen, USA (A-21202)	1:250

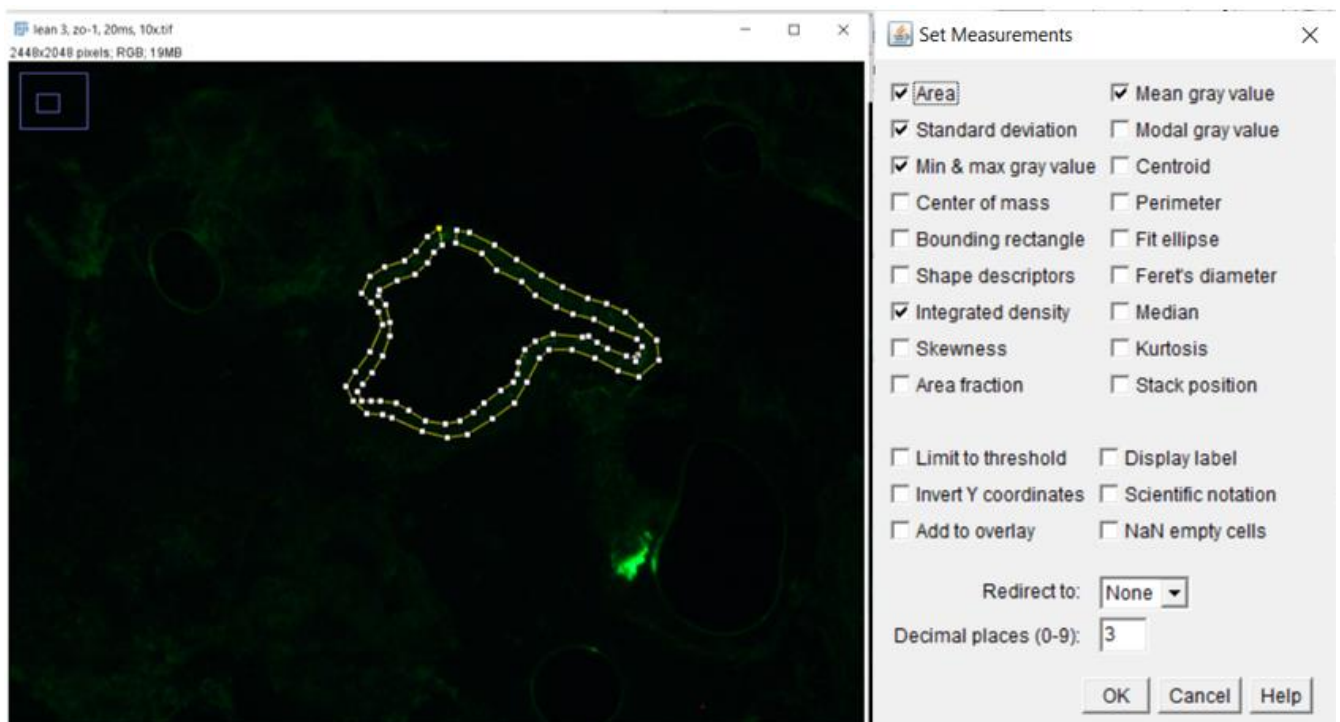


Figure 3.6: The measurements set in ImageJ and an example of how the aortas were analysed for the different fluorescent proteins.

3.4. Statistical analysis

Statistical analyses were performed using Statistica (TIBCO) and Graphpad prism (version 8). Shapiro-Wilk test was used to test the normality of the data sets. Normally distributed data sets were compared using standard t-tests, One-way and Two-way ANOVAs and Bonferroni post hoc tests. For non-parametric data sets, Kruskal-Wallis and Dunn's post hoc tests were performed. The level of statistical significance was set at $P < 0.05$. Data is represented as the mean \pm SD.

CHAPTER 4

4. RESULTS

4.1. The adult zebrafish model

Representative images of adult zebrafish size at experimental endpoint are presented in Figure 4.1, illustrating that the overfeeding protocol induced mild gain in body mass, rather than gross obesity. This is confirmed by the relative (37.7%), but significant increase in body mass and BMI compared to controls (Figure 4.2 and 4.4b) (mean body mass values for lean and overfed groups are 492.319 and 677.966 respectively), which validates this protocol as effective in inducing an overweight phenotype.

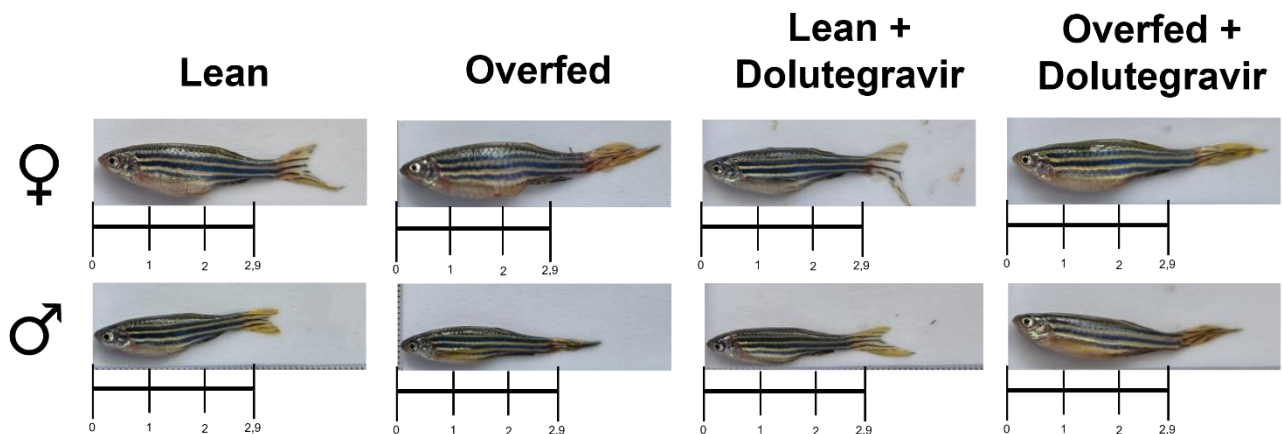


Figure 4.1: Representative images indicating the size of the adult zebrafish captured after euthanasia and weighing. The average length of an adult zebrafish is 2.9 cm ($\pm 0,2098$). The top row shows female zebrafish and the bottom row, male zebrafish.

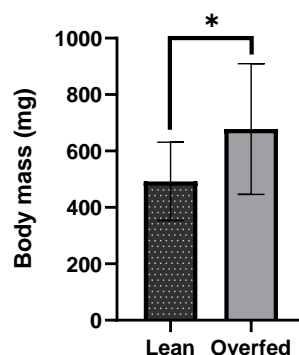


Figure 4.2: Body mass (mg) of adult zebrafish comparing lean and obese groups. $N=12$ per group. Statistical analysis: unpaired t -test and Bonferroni post hoc test. Data represented as mean \pm SD. * = $p=0,0317$.

In terms of DTG treatment, no significant effect was observed in either the lean or overfed groups in terms of body mass as represented in Figure 4.3. There was a 9.4% increase in body mass when comparing the lean and lean DTG group, however, this tendency was not seen in the comparison between overfed and overfed DTG group.

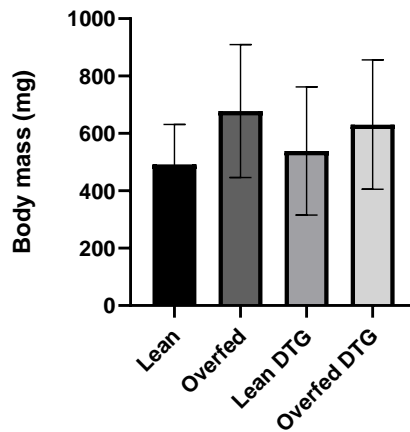


Figure 4.3: Body mass (mg) of adult zebrafish from the four different groups. $N=12$ per group. Statistical analysis: Kruskal-Wallis test and a Dunn's post hoc test. Data represented as mean \pm SD. DTG: Dolutegravir.

When accounting for the lengths of the fish (Figure 4.4 a), there was a significant difference in body mass when comparing the lean and overfed groups. Regarding the BMI of the zebrafish, there was also a significant increase in BMI of the overfed group when compared to the lean group (Figure 4.4 b).

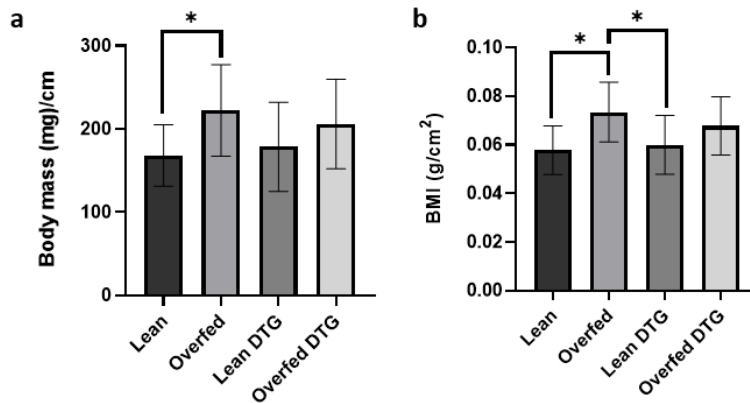


Figure 4.4: a) The body mass of the zebrafish per length (cm) and the b) BMI of the adult zebrafish. $N=12$ per group. Kruskal-Wallis test and Dunn's post hoc test. Data represented as mean \pm SD. $P<0,05$.

In terms of potential effect on redox outcome (liver H_2O_2 levels) there was no significant difference between the 4 groups (Figure 4.5.). However, the requirement to pool livers in groups of 2 due to their small size (i.e., $n=3$ per group) decreased statistical power, so that this outcome may not be conclusive. Indeed, an average 29.4% decrease was observed when comparing the lean (control) and lean DTG group, with a similar but somewhat smaller decrease of 23.2% in the overfed groups.

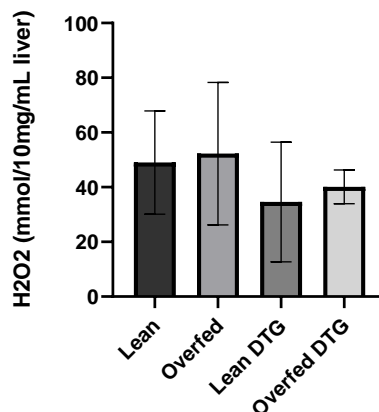


Figure 4.5: H_2O_2 (mmol/L/10 mg/mL liver) measured from the adult zebrafish livers. Two livers were pooled, $n=3$ per group. Statistical analysis: One-way ANOVA and Bonferroni post hoc test. Data represented as mean \pm SD. DTG: Dolutegravir

Turning attention to junction protein expression, the original aim was to assess this in the bulbous arteriosus – the zebrafish “equivalent” of the human ascending aorta - as this is an easy landmark to identify in zebrafish. However, as indicated in the representative image (Figure 4.6 a and b), it was difficult to distinguish the vessel wall from adjacent tissue. Given the fact that demarcation of the area for image analysis is always a somewhat subjective decision, the decision was taken to rather perform this analysis in the dorsal aorta, which was easier to demarcate accurately (Figure 4.7). Additionally, the brain was also harvested and stained to assess the tight and adherens junctions in the CNS, to compare this to the peripheral compartment. This was our first attempt at histological analysis of zebrafish brain tissue. At the point of our analyses, we were not confident that we could accurately standardise the area in which to measure the fluorescence in the brain vasculature (as seen in Figure 4.6 c and d) and it was therefore excluded from this study. However, with the right equipment, such as confocal microscopy, the assessment of the brain would be valuable to compare to the peripheral data in the future.

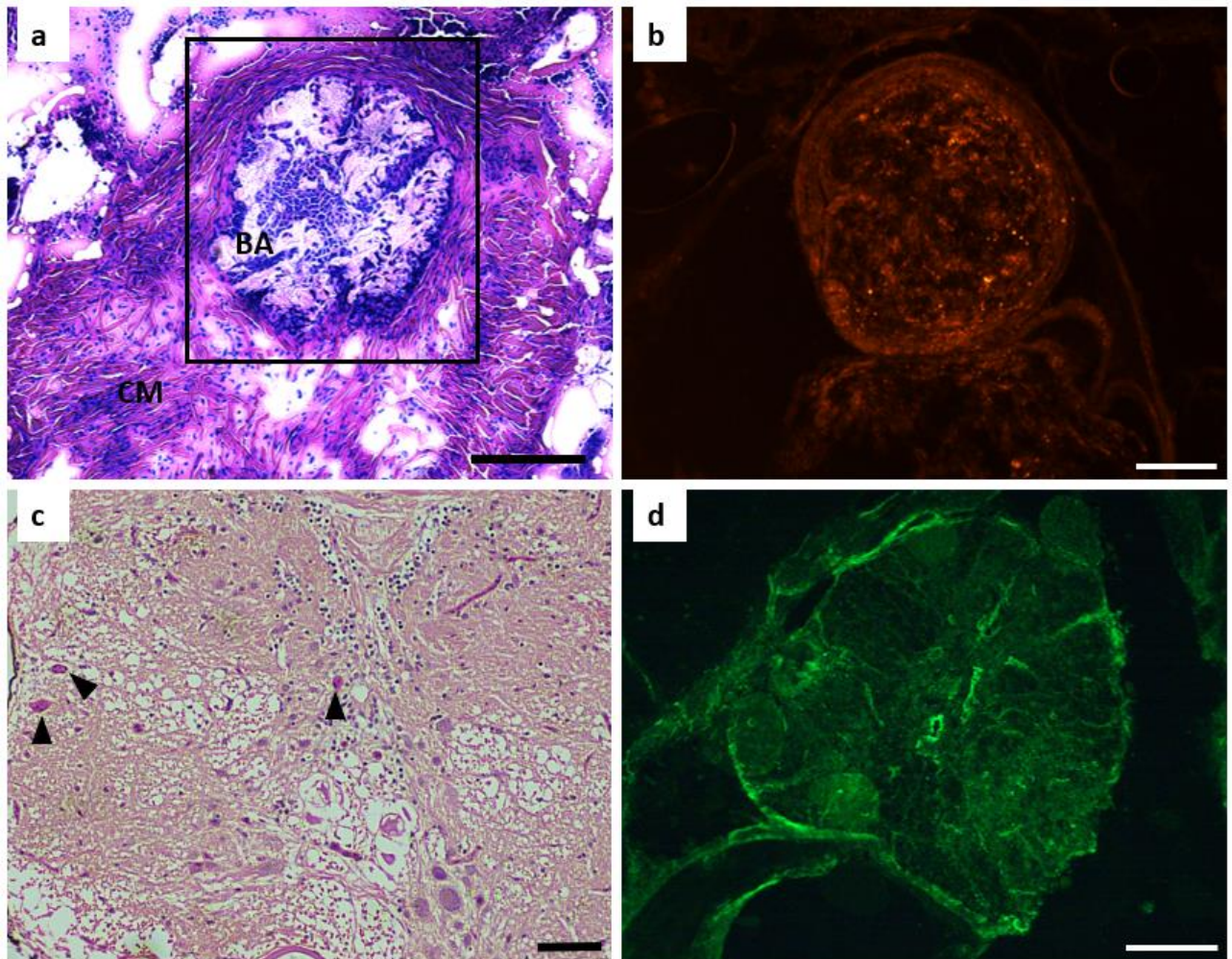


Figure 4.6: H&E stain of a transverse section of the a) adult zebrafish heart (scale bar: 100 μ m, magnification 10x plus the eyepiece magnification of 10x, total magnification: 100x)) and c) zebrafish brain, (scale bar: 50 μ m magnification 10x plus the eyepiece magnification of 10x, total magnification: 100x)) and fluorescence images of b) transverse section of the bulbus arteriosus of the zebrafish stained for claudin-5 (scale bar: 50 μ m, magnification 10x, plus the magnification of the eyepiece of 10x, thus total magnification of 100x) and d) transverse sections of the zebrafish brain stained for ZO-1 (scale bar: 50 μ m, magnification 10x, plus the magnification of the eyepiece of 10x, thus total magnification of 100x). Arrowheads indicate blood vessels, BA: Bulbus arteriosus CM: cardiac muscle.

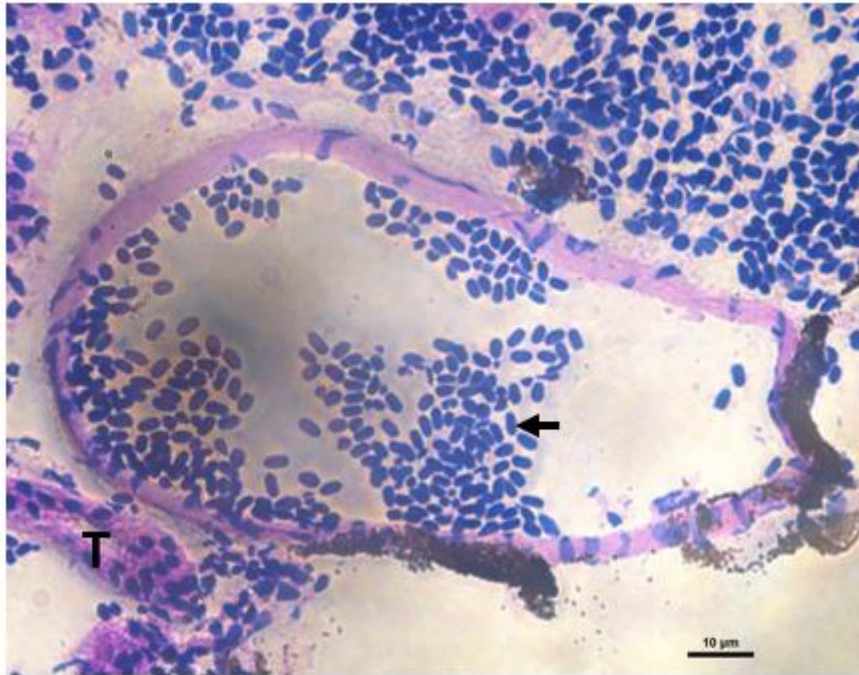


Figure 4.7: H&E section of a transverse 10 μm section of dorsal aorta of adult zebrafish (scale bar: 10 μm , magnification 60x plus the eyepiece magnification of 10x, total magnification: 600x). Arrow: Red blood cells, T: Tubule of kidney.

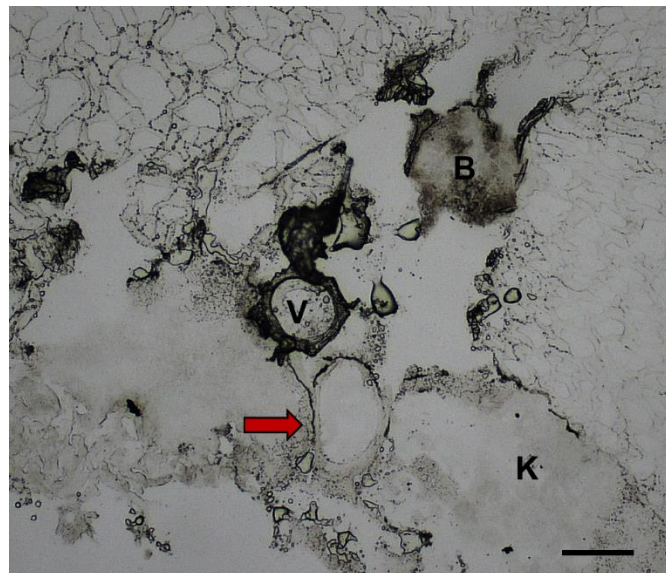


Figure 4.8: Brightfield images demonstrated how the dorsal aorta was located, using the position of the brain (B) and the vertebra (V). Red arrow: Dorsal aorta. K: kidney tissue. Magnification: 4x, plus the magnification of the eyepiece 10x (total magnification is 40x). Scale bar represents 100 μm .

Representative fluorescence images depicting protein expression of claudin-5, VE-cadherin and ZO-1 in the dorsal aorta, as well as quantified data, are presented in Figure 4.9. There was no significant difference between the claudin-5 or ZO-1 protein expression between the DTG treatment or overfeeding groups. When either overfeeding or treating with DTG in isolation, non-significant decreases were observed in VE-cadherin when compared to lean controls. However, a significant ANOVA main effect (ψ) of treatment was seen ($p < 0.05$). Additionally, the combination of overfeeding and DTG treatment resulted in a tendency for downregulation of VE-cadherin ($p = 0.0644$).

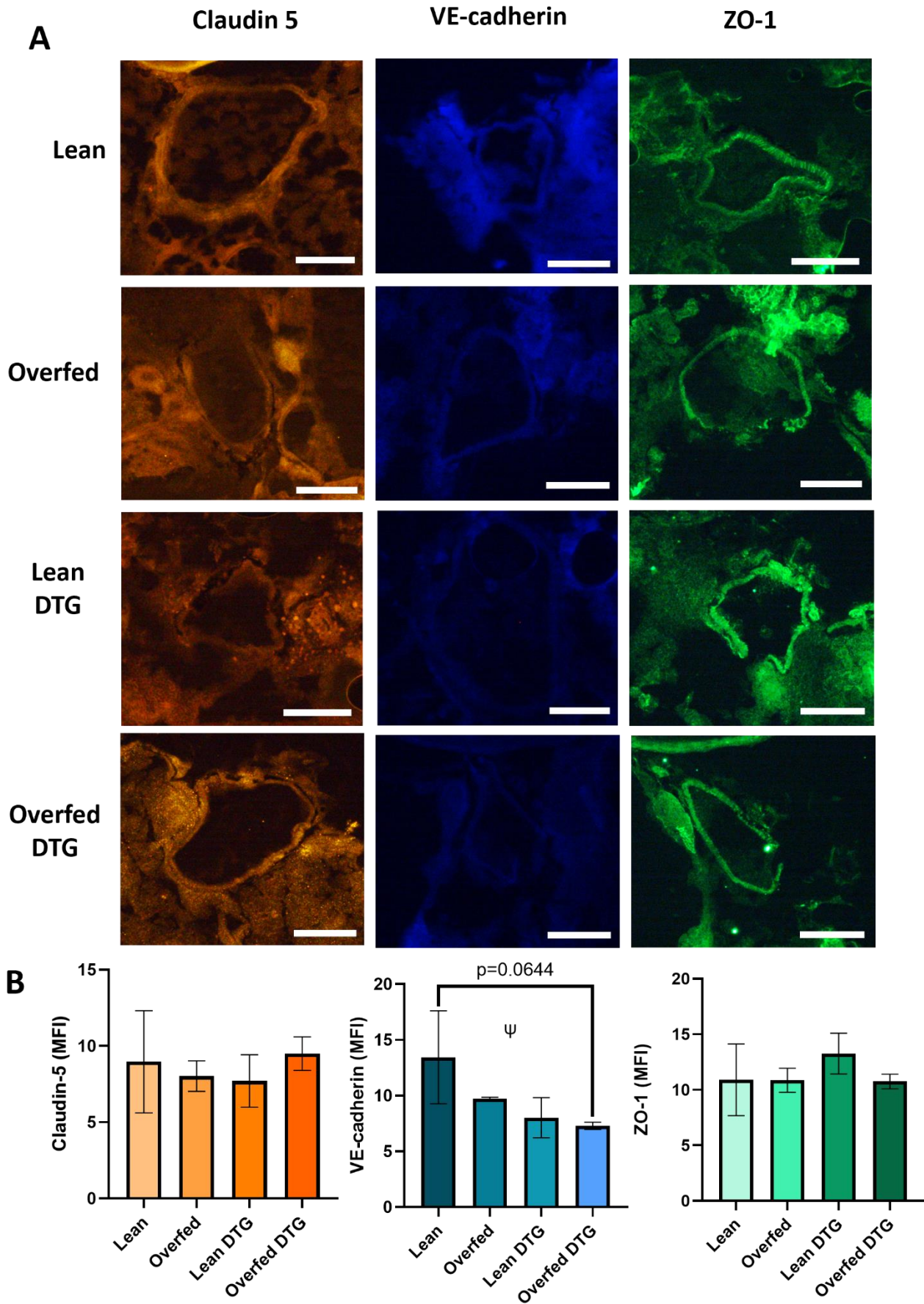


Figure 4.9: Image analysis of tight and adherens junctions in adult zebrafish dorsal aorta. A) Representative images of Claudin 5, VE-cadherin and ZO-1 in the different groups. B) The mean fluorescence intensity (MFI) of the tight and adherens junction proteins assessed in adult zebrafish dorsal aorta. $n=3$ per group. Statistical analysis: One-way ANOVA and bonferonni post hoc and multiple t - test. Data are shown as the mean \pm SD. Magnification 10x plus 10x magnification of the eyepiece (total magnification 100x): Scale bar represents 50 μ m. Ψ : ANOVA main effect of treatment ($p<0.05$).

4.2. The rat model

The baseline body mass of male and female rats for both intervention groups were the same at the starting point of the study (seen in Figure 4.10). There were no significant differences between control and treatment groups in terms of endpoint body mass. The expected significantly higher body mass in males compared to females was however evident ($p<0.0001$); Figure 4.11).

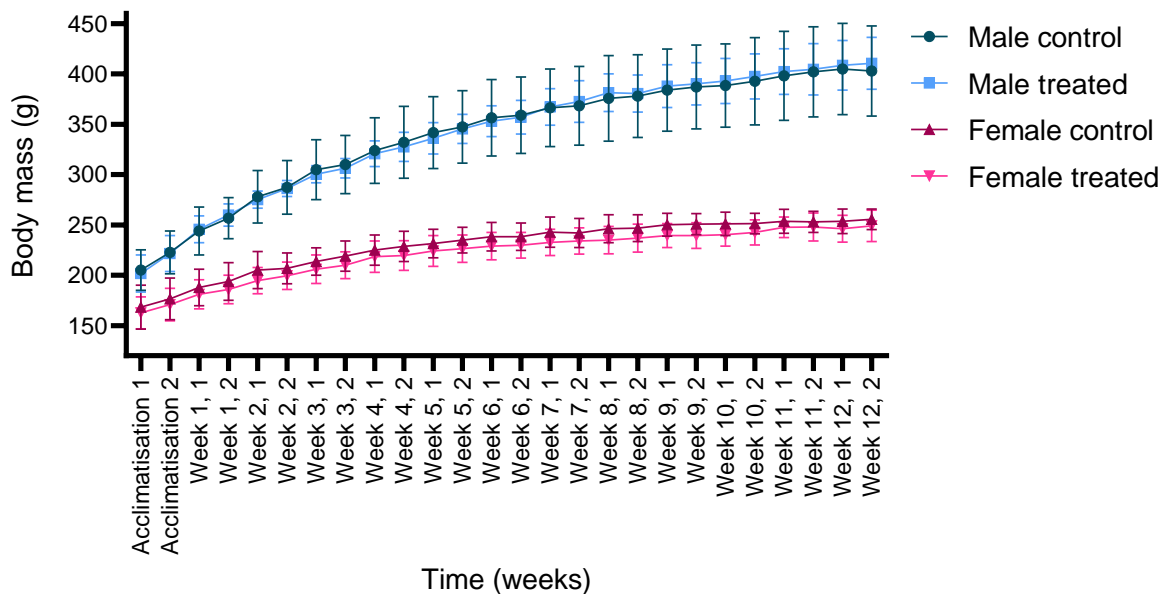


Figure 4.10: The body mass of male and female Wistar rats over the period of the 12-week DTG study. Body mass were measured twice a week and depicted as such. DTG: Dolutegravir.

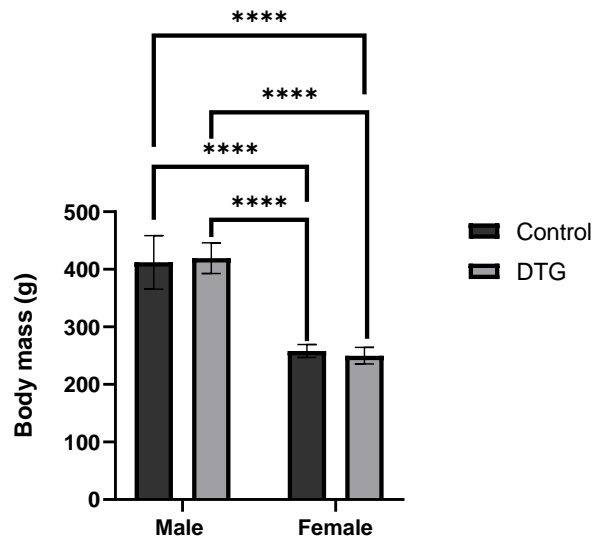


Figure 4.11: Body mass (g) of rats at the end of the study. $N=6$ per group. Statistical analysis: Two-way ANOVA and Bonferroni post hoc test. Data represented as mean \pm SD. ****= $p<0.0001$. DTG: Dolutegravir.

There was no significant difference in fasting blood glucose levels between the treated and control rats. It also ranged within the normal range of blood glucose levels for fasted rats.

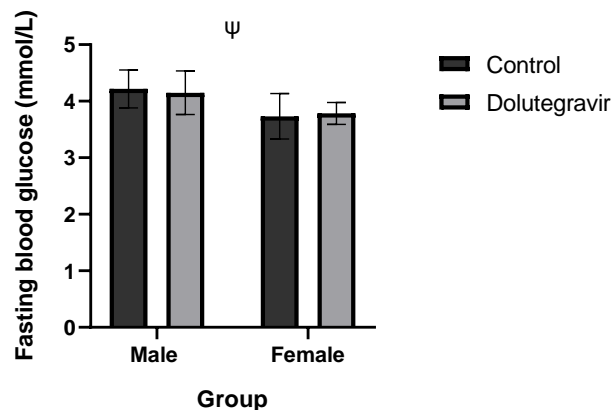


Figure 4.12: The fasting blood glucose at the endpoint of the study. $N=6$ per group. Two-way ANOVA and Bonferroni post hoc test. Data represented as mean \pm SD. Ψ : Significant ANOVA effect on sex, $p=0,0061$. DTG: Dolutegravir.

There was no significant difference between the liver weights of the treated and control groups (Figure 4.13a). Although there was a significant sex difference ($p<0.0001$), when correcting for the larger body mass in males, this difference was no longer evident (Figure 4.13b).

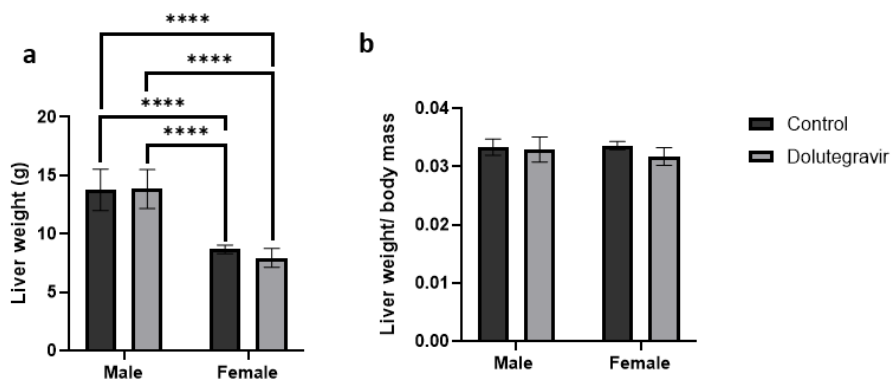


Figure 4.13: Rodent liver weight. a) The weights of the livers of the rats after harvesting and b) the weights of the livers corrected for body mass. $N=6$ per group. Statistical analysis: Two-way ANOVA and Bonferroni post hoc test. Data represented as mean \pm SD.

There was no difference between liver H_2O_2 in response to DTG treatment between control and treatment groups. An ANOVA effect on sex ($p=0.0026$) were seen and a tendency difference between male control and female control is evident ($p=0.0660$).

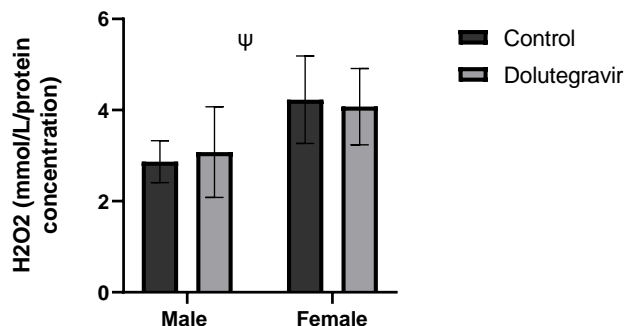


Figure 4.14: The H_2O_2 (mmol/L/protein concentration) measured from the rat livers. $N=6$ per group. Statistical analysis: Two-way ANOVA and Bonferroni post hoc test. Data represented as mean \pm SD. Ψ : Significant ANOVA effect on sex, $p=0.0026$

Similar practical challenges were experienced with processing of the rat tissue sections. Although we are experienced in analysis of brain tissue of rodents - as demonstrated in Figure 4.15 (a and b) – we lacked sufficiently sensitive equipment (such as a confocal microscope) to allow for accurate blood vessel location in the brain; thus, it was decided to exclude the

brain analysis for this study. These tissues will be stored until further and better analysis can be performed on them. We were however able to generate good quality data on the rat aorta (Figure 4.15 c).

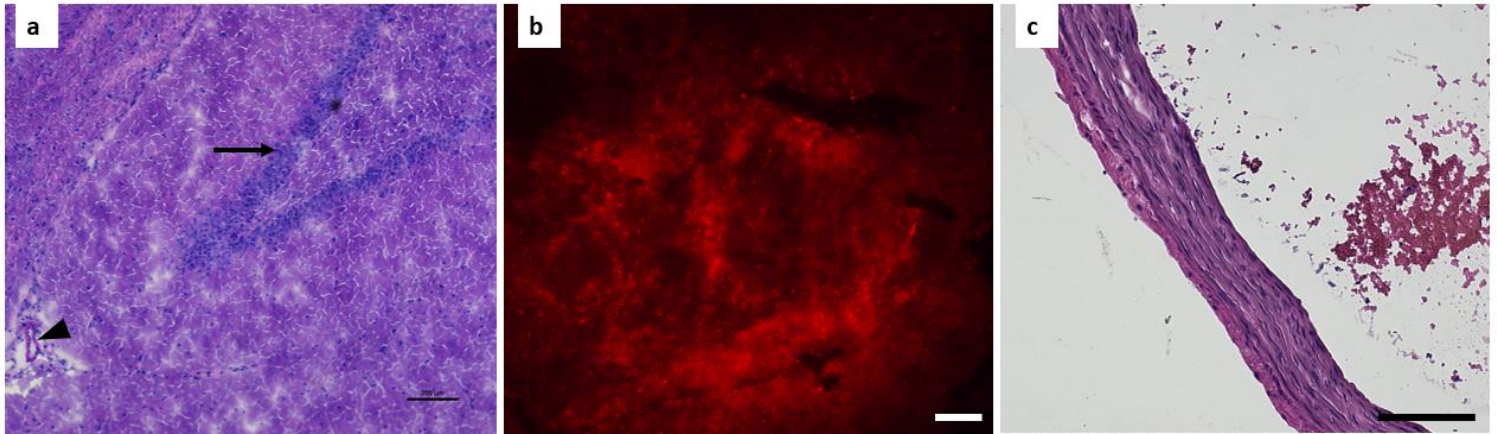


Figure 4.15: H&E stain of a transverse section of the a) rat mid brain (scale bar: 200 μm , magnification 4x plus the eyepiece magnification of 10x, total magnification: 40x) and b) fluorescence section of a c) rat aorta (scale bar: 100uM magnification 10x plus the eyepiece magnification of 10x, total magnification: 100x), Arrowhead: Blood vessel, Arrow: Hippocampal region of the brain.

Representative fluorescence images depicting protein expression of claudin-5, VE-cadherin and ZO-1 in the rat aorta, as well as quantitated data, are presented in Figure 4.16. There was no significant difference in the claudin-5 and VE-cadherin protein expression between the control and treatment groups. There was no significant difference in the expression of ZO-1 protein between treatment and control groups, however, there was a significant difference between male and female control groups ($p < 0.05$).

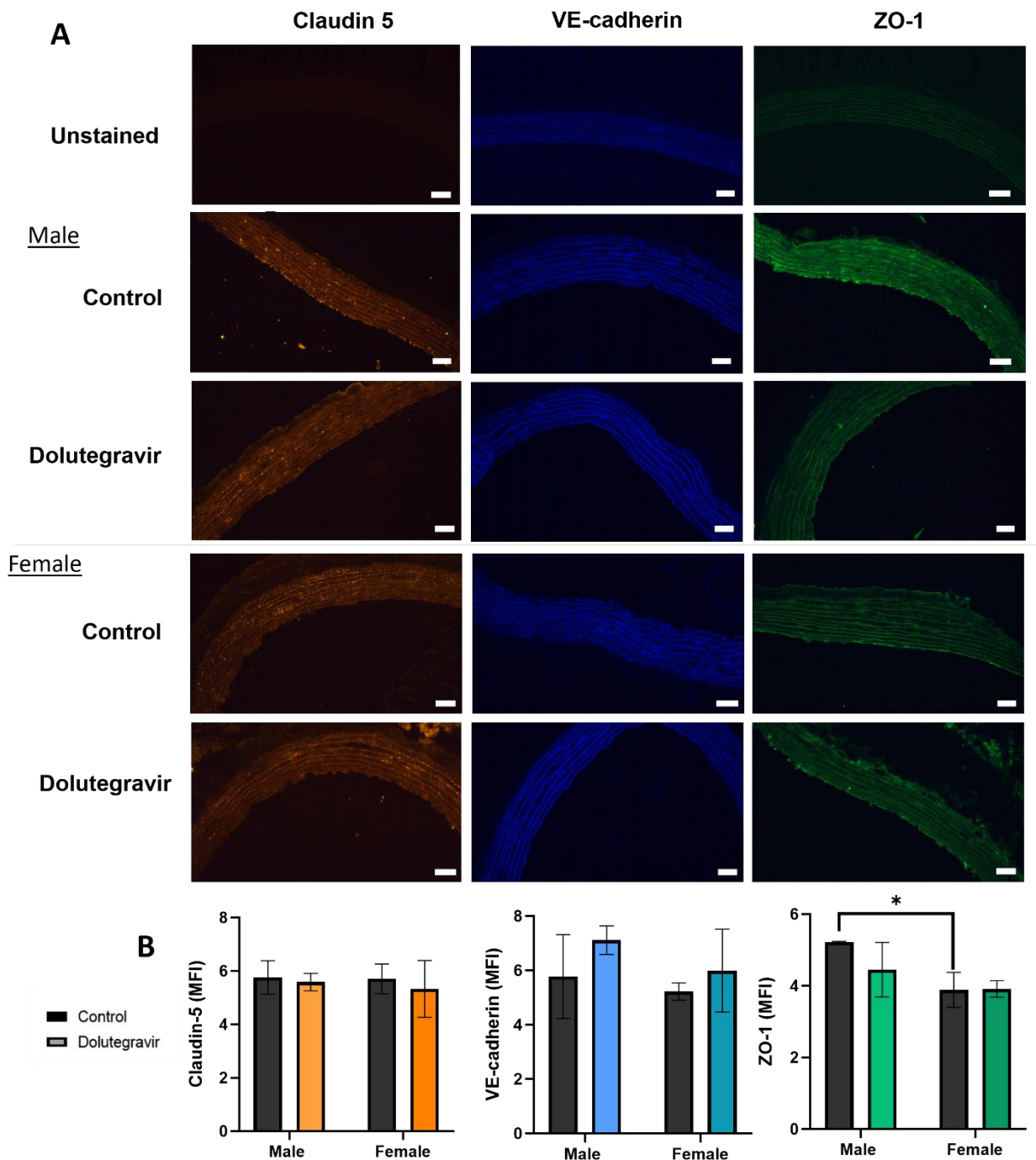


Figure 4.16: Image analysis of tight and adherens junctions in the rat aorta. A) Representative images of Claudin 5, VE-cadherin and ZO-1 in the different groups. B) The mean fluorescence intensity (MFI) of the tight and adherens junction proteins assessed in rat aorta. $n=3$ per group. Statistical analysis: One-way ANOVA and Bonferroni post hoc test. Data represented as mean \pm SD. Magnification 10x plus 10x magnification of the eyepiece (total magnification 100x). Scale bar represents 50 μ m.

CHAPTER 5

5. DISCUSSION

DTG has been associated with side effects such as weight gain, hyperglycaemia and neurological dysfunction (de Boer *et al.*, 2016; Hoffmann and Llibre, 2019; Kolakowska *et al.*, 2019; Menard *et al.*, 2017). However, there were some discrepancies in literature regarding a number of these side effects and the dosage of DTG making the understanding of this intervention unclear and requiring further elucidation. Therefore, we sought out to investigate the effect of chronic DTG administration on different aspects including vascular integrity and oxidative stress in rodents and adult zebrafish in the absence of the HI virus. In terms of potential mechanisms, this study aimed to investigate whether DTG is associated with endothelial dysfunction and increased ROS, as well as whether weight gain is a potential confounder.

5.1. The effects of Dolutegravir

DTG had no significant effect on the body mass of zebrafish and rodents in our study. This is the opposite of what literature and clinical studies indicate, as they show that DTG causes an increase in BMI (Gorwood *et al.*, 2020; Norwood *et al.*, 2018). Many studies also report females to be more susceptible to this increase in body mass (Bakal *et al.*, 2018; Venter *et al.*, 2019). This was not the case in the female rats in our study. These seemingly contradictory results may be explained. Firstly, it is important to note that the reported weight gain associated with DTG has been linked to an increase in appetite (Domingo *et al.*, 2020) when administered in high doses (McMahon *et al.*, 2020). In our study, where animals were not infected and therefore did not exhibit sickness-associated loss of appetite, there was little capacity for a “return to normal” increase in appetite. Secondly, some studies hypothesised that a higher degree of viral suppression might be the cause of the weight gain (Herrin *et al.*, 2016). This suggests that the interplay between DTG and the risk factors associated with the virus (low grade inflammation and immune activation) may be the cause of weight gain and diabetes. Our data thus suggest that DTG on its own, likely does not result in sufficient immune activation to result in a gain in body mass, as least not in the timespan our protocol assessed. It is also important to note that the literature which indicates weight gain, mostly report on combination treatment studies of DTG (Bourgi *et al.*, 2020; Norwood *et al.*, 2018). Although the other ARV drugs in the combination therapy therefore could be the reason for differences in the results. The literature regarding the weight gain phenomenon in DTG monotherapies

compared to combination therapies are sparse, as DTG monotherapy has been seen as inferior to decrease viral load compared to combination therapy (virological failure) (Fournier *et al.*, 2022; Hocqueloux *et al.*, 2019; Wijting *et al.*, 2017). Although the current study employed a relatively long intervention duration, it may be necessary to extend the duration of DTG administration even more in order to allow for firm conclusions to be made in this regard. This is important as tight junction expression differs between acute and chronic inflammation (Claesson-Welsh *et al.*, 2021). However, given the role of infection and appetite in weight gain, assessment of total body mass is probably not a sufficiently sensitive marker for use in non-infectious models. Rather, blood and tissue markers should be considered.

In terms of blood glucose levels in the rats, there was no sign of hyperglycemia, contradicting what most literature states (Gorwood *et al.*, 2020; McLaughlin *et al.*, 2018). According to most clinical studies and a parallel study done in humans and macaques, DTG causes an increase in insulin resistance and or hyperglycemia, due to increased adipose size, the toxicity of DTG on adipose tissue and the fact that DTG causes increased ROS levels. It has also been shown that DTG chelates magnesium and thereby increased insulin resistance (Hirigo *et al.*, 2022) However, in contrast to these reports, Auclair *et al.*(2020) and Afonso *et al.*, (2020) demonstrated that lower dose DTG administration (3.7 µg/ml, similar to what we employed) improved insulin sensitivity. It is therefore possible that effects of DTG is dose sensitive. A pharmacokinetics study – and assessment of tissue levels of DTG – may shed more light on the reason for these contradictory results. Due to the difficulty of acquiring sufficient blood for measuring fasting blood glucose in zebrafish, the blood glucose levels were not measured in the zebrafish model.

In terms of ROS, this study showed that DTG had no significant effect on the ROS levels of both zebrafish and rats. However, in the zebrafish, there was a 29.5% decrease in ROS between the lean and lean DTG zebrafish groups and a 23.2% decrease between the overfed and overfed DTG group (assessing only the effect of DTG). As there are some discrepancies in literature, the results agree with some of the literature that states DTG has no effect on ROS levels (Afonso *et al.*, 2017; Auclair *et al.*, 2020) and showed anti-inflammatory effects. An *in vivo* study done by Gorwood *et al.* (2020) showed that DTG (3.1 µg/mL) increased ROS and mitochondrial dysfunction in proliferating ASCs. Our results portray ROS levels as found in the liver, as the liver is the organ responsible for the most metabolic activity in the whole organism (Méndez *et al.*, 2017). The antioxidant capacity of the liver and of adipose tissue might not be the same. A study that associated increased weight gain with increased levels of ROS (Gorwood *et al.*, 2020) was only measured by increased adipose size and lipid accumulation (not human weight gain), and visceral fat vs subcutaneous fat increases were not measured. It is not clear whether or not DTG increases human visceral or subcutaneous

fat, and as they have different metabolic implications it is necessary to distinguish between the two. ROS is mostly associated with visceral adipose tissue.

In terms of junction proteins, the administration of DTG did not change the expression of ZO-1 and Claudin-5 in both the zebrafish and rodent models used. It is important to note that tight junction and adherens junction molecules have different responsibilities and “act” differently in different organs, depending on the permeability required (Dejana *et al.*, 2009.). Literature on ZO-1 in the aorta specifically is scarce and most literature is about ZO-1 and its role in the BBB (Branca *et al.*, 2019; Hirase *et al.*, 1997), which means that the effect of ZO-1 is visualised less in these regions. The low expression observed in claudin-5 in the aortas may be due to claudin being predominantly expressed in the BBB and is not as involved in the integrity of the endothelium in the large arteries (Li *et al.*, 2022) and therefore will make the detection of small changes less likely. A study done on the effect of DTG on the BBB showed that DTG caused a decrease in claudin-5 expression (Ma *et al.*, 2020). However, this study was done *in vitro* and with the concentration of 25 μM (this roughly translates to 10.5 $\mu\text{g/mL}$ of DTG) and is thus more than 3 times the human equivalent dose (3.33 $\mu\text{g/mL}$ for 15 L body fluid). This shows the importance to include both peripheral and central compartments of an organism to see the whole effect of the drug on both compartments. In future studies it would be recommended to assess the endothelial integrity in the CNS region. VE-cadherin showed no significant difference in the rat model. However, in the zebrafish model there was an ANOVA main effect of treatment on VE-cadherin expression in the zebrafish aorta. While DTG treatment alone was not sufficient to illicit a significant VE-cadherin response, there was a trend for a cumulative effect of overfeeding and DTG intervention in the zebrafish, which will be discussed further in the next section. A decrease in VE-cadherin is associated with the phosphorylation of tyrosine (Dejana and Vestweber, 2013). This is usually caused by ROS and pro-inflammatory cytokines (Colás-Algora *et al.*, 2020). It has been shown that inhibiting NF- κB leads to the decrease of VE-cadherin and thus increased endothelial cell-permeability (Colás-Algora *et al.*, 2020). Research has shown that DTG causes a decrease in the expression of NF- κB (Auclair *et al.*, 2020), thereby contributing to endothelial permeability. There is a constant need for endothelial barrier permeability homeostasis. A study showed that endothelial cells, especially those from large vessels such as HUVECs, have molecular mechanisms in place to ensure there are sufficient VE-cadherin molecules at the plasma membrane in order to preserve barrier integrity. This is even the case when endothelial barrier permeability is increased, and adherens junctions are transiently destabilized in an inflammatory scenario. That study also showed that TNF α -mediated VE-cadherin degradation can be compensated by an increase of VE-cadherin synthesis (Colás-Algora *et al.*, 2020). Assessment of cytokine profile was not within the scope of the current study, but such

assessment would significantly contribute to interpretation of data. The compensatory mechanisms may explain why there is no difference in the rat VE-cadherin levels and measuring these in a longitudinal study with repeated measures at multiple different time points may give better insight into the homeostasis mechanisms.

5.2. The effects of Obesity as potential confounder

The effect of obesity was investigated through means of an overfeeding model in zebrafish. The significant difference in BMI between lean and overfed zebrafish groups validates the overfeeding model. When considering effects of DTG, overfed fish did not differ from lean ones in terms of body mass response. Similarly, the overfeeding of the zebrafish did not have an effect on the hydrogen peroxide levels, as the difference between lean and overfed groups were not significant (6.67% increase, $p > 0,9999$). A study done on the difference between HFD and NFD in zebrafish showed that there were larger visceral and smaller subcutaneous adipocytes, elevated blood glucose and triglyceride levels in HFD zebrafish when compared to the NFD zebrafish (Faillaci *et al.*, 2018). Together, these data suggest that depending on the type of diet given to the fish, the metabolic outcome might differ from “healthy weight gain” or “unhealthy weight gain”. In the current study, zebrafish were overfed on a normal diet (i.e. not high fat), which may account for the stable ROS levels observed. Additionally, the increased adiposity shows that overfeeding might exacerbate the effects seen in the tight junction protein expression. The decrease in VE-cadherin levels of the lean vs overfed DTG group were near significant ($p=0.06$), suggesting a potential cumulative effect of overfeeding and DTG. As seen in literature, DTG administration did not increase (Auclair *et al.*, 2020) and even decreased (Afonso *et al.*, 2017) soluble intracellular cell adhesion molecule-1 (sICAM-1) and soluble vascular cell adhesion molecule-1 (sVCAM-1). This finding in addition to the findings of a decrease in inflammatory markers (such as IL-6), a decrease in endothelial cellular senescence and an increase in eNOS levels (Afonso *et al.*, 2017), indicate that the effect seen on VE-cadherin must be influenced by the effect of obesity, as DTG on its own does not seem to have an effect on the fluorescence levels of VE-cadherin. This is confirmed by the current rat study, where obesity was not a confounder. In this study’s circumstances, the HFD-induced rats showed adverse effects, which could cause confounding results and were therefore excluded. Even though, the overfeeding model did not show increased ROS levels and may thus be associated with metabolically healthy obesity findings, metabolically obese individuals still have increased adhesion molecules compared to lean individuals (Mulhem *et al.*, 2021). An increase of adhesion molecules have been associated with a decrease in VE-cadherin expression, increased endothelial permeability and subsequent

transmigration of leukocytes (Kovacs *et al.*, 2022). In future it would be interesting to see if this same effect would be seen in the rats. The fact that obesity showed a tendency to decrease the levels of expression of VE-cadherin (one of the main adherens junction proteins responsible for the permeability of the endothelial barrier) may impact human research in the South African context, as a high number of individuals are obese and/or have HIV. The synergistic effect of obesity may cause serious detrimental effects in terms of endothelial dysfunction. Seen as endothelial dysfunction is one of the main risk factors for diabetes, CVD and atherosclerosis, VE-cadherin should be further investigated as potential therapeutic target to prevent the endothelial dysfunction known to increase co-morbidity risk in HIV.

5.3. Comparison of zebrafish and rat models

When considering the suitability of zebrafish as a model for the investigation of the effects of DTG and obesity in the current context in particular, the 9.4% body mass increase between the lean and lean DTG group, show that zebrafish demonstrate increased sensitivity to reflect effects of DTG compared to rodents. According to the FDA, a 5% increase in body mass is considered significant (“Guidance for Industry Developing Products for Weight Management,” 2007), which confirms the clinical relevance of increased body mass induced by DTG intervention. When comparing our results to that of other relevant literature, a much smaller effect of DTG on body mass has been reported in other studies after overfeeding, with a recent report demonstrating a 3% increase following DTG treatment (Sax *et al.*, 2020). When looking at the overfed vs overfed DTG group, the increase in weight was not significant and can be supported by a study which stated that there were no measurable difference in the rates of change in BMI before and after DTG transition in individuals who were overweight or obese prior to DTG treatment (Thivalapill *et al.*, 2021). In terms of ROS, the 29.5% decrease in H₂O₂ levels between the lean and lean DTG group (only considering the effect of DTG) in the zebrafish – in comparison to no observed effect in rats - may indicate that the zebrafish has an inherent active antioxidant defense system which actively decreased the elevated levels of ROS to a lower-than-normal level. This difference might be explained by species differences in capacity of endogenous antioxidant defense mechanisms. However, literature indicates that zebrafish show similarities across the antioxidant defense systems compared to those of mammalian organisms (Massarsky *et al.*, 2017). Thus, further research is required to confirm that the dose used in zebrafish correspond to the dose used in rats (when e.g., considering differences in metabolic rate and drug breakdown/clearance), before firm conclusion can be made on whether or not the zebrafish model may be a more sensitive model. However, given

the current results and the relatively lower cost of zebrafish models, this option warrants further exploration.

Our study has some limitations. The expression of tight and adherens junctions on the surface of the endothelial cell and internalized tight junctions could not be distinctly separated in this study. Higher resolution visualisation equipment is needed to capture the finer detail in terms of endothelial tight and adherens junctions in between endothelial cells. Furthermore, little research has been done on the tight junctions in adult zebrafish. Most research on tight junctions is done on larvae as they are transparent and thus make the visualisation of the tight junctions easier. However, zebrafish larvae and adult vasculature is disparate, as they still develop immensely over period of months (Miano *et al.*, 2006) and the research done on the larvae can therefore not be used comparatively with studies done on adult zebrafish. Thus, the research done on adult zebrafish is novel and will need some more investigation.

5.4. Conclusion

In summary, data presented suggest that DTG does not cause significant detrimental effects in terms of weight gain, ROS levels or endothelial junction protein expression profile in the absence of obesity. However, in the presence of overfeeding, it seemed to have a cumulative effect on the expression of VE-cadherin, which indicate increased endothelial permeability. This is an important finding as a large proportion of our current population of PLWH are overweight or obese. Since relatively recent evidence suggests that adipocytes may harbour the HI-virus (Couturier *et al.*, 2018; Damouche *et al.*, 2015) making the use of ARVs such as DTG an increased risk to obese patients, our data significantly contributes to our understanding of the potential risks associated with DTG treatment.

6. REFERENCES

- Abraham, S.B., Rubino, D., Sinaii, N., Ramsey, S., Nieman, L.K., 2013. Cortisol, obesity, and the metabolic syndrome: A cross-sectional study of obese subjects and review of the literature: Cortisol and Metabolic Syndrome. *Obesity* 21, E105–E117. <https://doi.org/10.1002/oby.20083>
- Adan, R.A.H., Tiesjema, B., Hillebrand, J.J.G., la Fleur, S.E., Kas, M.J.H., de Krom, M., 2006. The MC4 receptor and control of appetite: The MC4 receptor and control of appetite. *British Journal of Pharmacology* 149, 815–827. <https://doi.org/10.1038/sj.bjp.0706929>
- Afonso, P., Auclair, M., Caron-Debarle, M., Capeau, J., 2017. Impact of CCR5, integrase and protease inhibitors on human endothelial cell function, stress, inflammation and senescence. *Antivir Ther* 22, 645–657. <https://doi.org/10.3851/IMP3160>
- Alaba, O., Chola, L., 2014a. Socioeconomic Inequalities in Adult Obesity Prevalence in South Africa: A Decomposition Analysis. *IJERPH* 11, 3387–3406. <https://doi.org/10.3390/ijerph110303387>
- Alaba, O., Chola, L., 2014b. Socioeconomic inequalities in adult obesity prevalence in South Africa: A decomposition analysis. *International Journal of Environmental Research and Public Health* 11, 3387–3406. <https://doi.org/10.3390/ijerph110303387>
- Alam, I., Ng, T.P., Larbi, A., 2012. Does Inflammation Determine Whether Obesity Is Metabolically Healthy or Unhealthy? The Aging Perspective. *Mediators of Inflammation* 2012, 1–14. <https://doi.org/10.1155/2012/456456>
- Andreicuț, A., Cătoi, A., Cătoi, C., Crăciun, A., Mironiuc, A., Pârvu, A., Pop, I., 2018. Metabolically Healthy versus Unhealthy Morbidly Obese: Chronic Inflammation, Nitro-Oxidative Stress, and Insulin Resistance. *Nutrients* 10, 1199. <https://doi.org/10.3390/nu10091199>
- Auclair, M., Guénantin, A.-C., Fellahi, S., Garcia, M., Capeau, J., 2020. HIV antiretroviral drugs, dolutegravir, maraviroc and ritonavir-boosted atazanavir use different pathways to affect inflammation, senescence and insulin sensitivity in human coronary endothelial cells. *PLoS ONE* 15, e0226924. <https://doi.org/10.1371/journal.pone.0226924>
- Bakal, D.R., Coelho, L.E., Luz, P.M., Clark, J.L., De Boni, R.B., Cardoso, S.W., Veloso, V.G., Lake, J.E., Grinsztejn, B., 2018. Obesity following ART initiation is common and influenced by both traditional and HIV-/ART-specific risk factors. *Journal of Antimicrobial Chemotherapy* 73, 2177–2185. <https://doi.org/10.1093/jac/dky145>
- Baker, J., Ayenew, W., Quick, H., Hullsiek, K.H., Tracy, R., Henry, K., Duprez, D., Neaton, J.D., 2010. High-Density Lipoprotein Particles and Markers of Inflammation and

- Thrombotic Activity in Patients with Untreated HIV Infection. *J INFECT DIS* 201, 285–292. <https://doi.org/10.1086/649560>
- Bavinger, C., Bendavid, E., Niehaus, K., Olshen, R.A., Olkin, I., Sundaram, V., Wein, N., Holodniy, M., Hou, N., Owens, D.K., Desai, M., 2013. Risk of Cardiovascular Disease from Antiretroviral Therapy for HIV: A Systematic Review. *PLoS ONE* 8, e59551. <https://doi.org/10.1371/journal.pone.0059551>
- Benjamin, L.A., Bryer, A., Emsley, H.C., Khoo, S., Solomon, T., Connor, M.D., 2012. HIV infection and stroke: current perspectives and future directions. *The Lancet Neurology* 11, 878–890. [https://doi.org/10.1016/S1474-4422\(12\)70205-3](https://doi.org/10.1016/S1474-4422(12)70205-3)
- Bertrand, L., Velichkovska, M., Toborek, M., 2019. Cerebral Vascular Toxicity of Antiretroviral Therapy. *J Neuroimmune Pharmacol.* <https://doi.org/10.1007/s11481-019-09858-x>
- Bourgi, K., Rebeiro, P.F., Turner, M., Castilho, J.L., Hulgán, T., Raffanti, S.P., Koethe, J.R., Sterling, T.R., 2020. Greater Weight Gain in Treatment-naive Persons Starting Dolutegravir-based Antiretroviral Therapy. *Clinical Infectious Diseases* 70, 1267–1274. <https://doi.org/10.1093/cid/ciz407>
- Bradford, M.M., n.d. A Rapid and Sensitive Method for the Quantitation of Microgram Quantities of Protein Utilizing the Principle of Protein-Dye Binding 7.
- Branca, J.J.V., Maresca, M., Morucci, G., Mello, T., Becatti, M., Pazzagli, L., Colzi, I., Gonnelli, C., Carrino, D., Paternostro, F., Nicoletti, C., Ghelardini, C., Gulisano, M., Di Cesare Mannelli, L., Pacini, A., 2019. Effects of Cadmium on ZO-1 Tight Junction Integrity of the Blood Brain Barrier. *IJMS* 20, 6010. <https://doi.org/10.3390/ijms20236010>
- Broermann, A., Winderlich, M., Block, H., Frye, M., Rossaint, J., Zarbock, A., Cagna, G., Linnepe, R., Schulte, D., Nottebaum, A.F., Vestweber, D., 2011. Dissociation of VE-PTP from VE-cadherin is required for leukocyte extravasation and for VEGF-induced vascular permeability in vivo. *Journal of Experimental Medicine* 208, 2393–2401. <https://doi.org/10.1084/jem.20110525>
- Cahn, P., Pozniak, A.L., Mingrone, H., Shuldyakov, A., Brites, C., Andrade-Villanueva, J.F., Richmond, G., Buendia, C.B., Fourie, J., Ramgopal, M., Hagins, D., Felizarta, F., Madruga, J., Reuter, T., Newman, T., Small, C.B., Lombaard, J., Grinsztejn, B., Dorey, D., Underwood, M., Griffith, S., Min, S., 2013. Dolutegravir versus raltegravir in antiretroviral-experienced, integrase-inhibitor-naive adults with HIV: week 48 results from the randomised, double-blind, non-inferiority SAILING study. *The Lancet* 382, 700–708. [https://doi.org/10.1016/S0140-6736\(13\)61221-0](https://doi.org/10.1016/S0140-6736(13)61221-0)
- Cai, H., Harrison, D.G., 2000. Endothelial Dysfunction in Cardiovascular Diseases: The Role of Oxidant Stress. *Circulation Research* 87, 840–844. <https://doi.org/10.1161/01.RES.87.10.840>

- Claesson-Welsh, L., Dejana, E., McDonald, D.M., 2021. Permeability of the Endothelial Barrier: Identifying and Reconciling Controversies. *Trends in Molecular Medicine* 27, 314–331. <https://doi.org/10.1016/j.molmed.2020.11.006>
- Colás-Algora, N., García-Weber, D., Cacho-Navas, C., Barroso, S., Caballero, A., Ribas, C., Correas, I., Millán, J., 2020. Compensatory increase of VE-cadherin expression through ETS1 regulates endothelial barrier function in response to TNF α . *Cell. Mol. Life Sci.* 77, 2125–2140. <https://doi.org/10.1007/s00018-019-03260-9>
- Corrêa, Heyn, Magalhaes, 2019. The Impact of the Adipose Organ Plasticity on Inflammation and Cancer Progression. *Cells* 8, 662. <https://doi.org/10.3390/cells8070662>
- Cottrell, M.L., Hadzic, T., Kashuba, A.D.M., 2013. Clinical Pharmacokinetic, Pharmacodynamic and Drug-Interaction Profile of the Integrase Inhibitor Dolutegravir. *Clin Pharmacokinet* 52, 981–994. <https://doi.org/10.1007/s40262-013-0093-2>
- Couturier, J., Winchester, L.C., Suliburk, J.W., Wilkerson, G.K., Podany, A.T., Agarwal, N., Xuan Chua, C.Y., Nehete, P.N., Nehete, B.P., Grattoni, A., Sastry, K.J., Fletcher, C.V., Lake, J.E., Balasubramanyam, A., Lewis, D.E., 2018. Adipocytes impair efficacy of antiretroviral therapy. *Antiviral Research* 154, 140–148. <https://doi.org/10.1016/j.antiviral.2018.04.002>
- Cypess, A.M., Kahn, C.R., 2013. Brown fat as a therapy for obesity and diabetes. *Current Opinion in Endocrinology, Diabetes and Obesity* 14. <https://doi.org/10.1097/MED.0b013e328337a81f>
- Damouche, A., Lazure, T., Avettand-Fènoël, V., Huot, N., Dejucq-Rainsford, N., Satie, A.-P., Mélard, A., David, L., Gommet, C., Ghosn, J., Noel, N., Pourcher, G., Martinez, V., Benoist, S., Béréziat, V., Cosma, A., Favier, B., Vaslin, B., Rouzioux, C., Capeau, J., Müller-Trutwin, M., Dereuddre-Bosquet, N., Le Grand, R., Lambotte, O., Bourgeois, C., 2015. Adipose Tissue Is a Neglected Viral Reservoir and an Inflammatory Site during Chronic HIV and SIV Infection. *PLoS Pathog* 11, e1005153. <https://doi.org/10.1371/journal.ppat.1005153>
- de Boer, M.G.J., van den Berk, G.E.L., van Holten, N., Oryszcyn, J.E., Dorama, W., Moha, D. ait, Brinkman, K., 2016. Intolerance of dolutegravir-containing combination antiretroviral therapy regimens in real-life clinical practice. *AIDS* 30, 2831–2834. <https://doi.org/10.1097/QAD.0000000000001279>
- Dejana, E., Tournier-Lasserre, E., Weinstein, B.M., n.d. The Control of Vascular Integrity by Endothelial Cell Junctions: Molecular Basis and Pathological Implications. *Developmental Cell* 13.
- Dejana, E., Vestweber, D., 2013. The Role of VE-Cadherin in Vascular Morphogenesis and Permeability Control, in: *Progress in Molecular Biology and Translational Science*. Elsevier, pp. 119–144. <https://doi.org/10.1016/B978-0-12-394311-8.00006-6>

- Domingo, P., Villarroya, F., Giral, M., Domingo, J.C., 2020. Potential role of the melanocortin signaling system interference in the excess weight gain associated to some antiretroviral drugs in people living with HIV. *Int J Obes* 44, 1970–1973. <https://doi.org/10.1038/s41366-020-0551-5>
- Dominick, L., Midgley, N., Swart, L.-M., Sprake, D., Deshpande, G., Laher, I., Joseph, D., Teer, E., Essop, M.F., 2020. HIV-related cardiovascular diseases: the search for a unifying hypothesis. *American Journal of Physiology-Heart and Circulatory Physiology* 318, H731–H746. <https://doi.org/10.1152/ajpheart.00549.2019>
- Duong, C.N., Vestweber, D., 2020. Mechanisms Ensuring Endothelial Junction Integrity Beyond VE-Cadherin. *Front. Physiol.* 11, 519. <https://doi.org/10.3389/fphys.2020.00519>
- Eckard, A.R., McComsey, G.A., 2020. Weight gain and integrase inhibitors: Current Opinion in Infectious Diseases 33, 10–19. <https://doi.org/10.1097/QCO.0000000000000616>
- Faillaci, F., Milosa, F., Critelli, R.M., Turola, E., Schepis, F., Villa, E., 2018. Obese zebrafish: A small fish for a major human health condition. *Anim Models Exp Med* 1, 255–265. <https://doi.org/10.1002/ame2.12042>
- Fournier, A.L., Hocqueloux, L., Braun, D.L., Metzner, K.J., Kouyos, R.D., Raffi, F., Briant, A.R., Martinez, E., De Lazzari, E., Negredo, E., Rijnders, B., Rokx, C., Günthard, H.F., Parienti, J.-J., 2022. Dolutegravir Monotherapy as Maintenance Strategy: A Meta-Analysis of Individual Participant Data From Randomized Controlled Trials. *Open Forum Infectious Diseases* 9, ofac107. <https://doi.org/10.1093/ofid/ofac107>
- Furukawa, S., Fujita, T., Shimabukuro, M., Iwaki, M., Yamada, Y., Nakajima, Y., Nakayama, O., Makishima, M., Matsuda, M., Shimomura, I., 2004. Increased oxidative stress in obesity and its impact on metabolic syndrome. *J. Clin. Invest.* 114, 1752–1761. <https://doi.org/10.1172/JCI21625>
- Gannon, P., Khan, M.Z., Kolson, D.L., 2011. Current understanding of HIV-associated neurocognitive disorders pathogenesis. *Current Opinion in Neurology* 24, 275–283. <https://doi.org/10.1097/WCO.0b013e32834695fb>
- Gatell, J.M., Assoumou, L., Moyle, G., Waters, L., Johnson, M., Domingo, P., Fox, J., Martinez, E., Stellbrink, H., Guaraldi, G., Masia, M., Gompels, M., De Wit, S., Florence, E., Esser, S., Raffi, F., Pozniak, A.L., 2017. Switching from a ritonavir-boosted protease inhibitor to a dolutegravir-based regimen for maintenance of HIV viral suppression in patients with high cardiovascular risk. *AIDS* 31, 2503–2514. <https://doi.org/10.1097/QAD.0000000000001675>
- Ghaddar, B., 2020. Impaired brain homeostasis and neurogenesis in diet-induced overweight zebrafish: a preventive role from *A. borbonica* extract. *Scientific Reports* 17.

- Ghaddar, B., Veeren, B., Rondeau, P., Bringart, M., Lefebvre d'Hellencourt, C., Meilhac, O., Bascands, J.-L., Diotel, N., 2020. Impaired brain homeostasis and neurogenesis in diet-induced overweight zebrafish: a preventive role from *A. borbonica* extract. *Sci Rep* 10, 14496. <https://doi.org/10.1038/s41598-020-71402-2>
- Gómez-Hernández, A., Beneit, N., Díaz-Castroverde, S., Escribano, Ó., 2016. Differential Role of Adipose Tissues in Obesity and Related Metabolic and Vascular Complications. *International Journal of Endocrinology* 2016, 1–15. <https://doi.org/10.1155/2016/1216783>
- Gorwood, J., Bourgeois, C., Pourcher, V., Pourcher, G., Charlotte, F., Mantecon, M., Rose, C., Morichon, R., Atlan, M., Le Grand, R., Desjardins, D., Katlama, C., Fève, B., Lambotte, O., Capeau, J., Béréziat, V., Lagathu, C., 2020. The Integrase Inhibitors Dolutegravir and Raltegravir Exert Proadipogenic and Profibrotic Effects and Induce Insulin Resistance in Human/Simian Adipose Tissue and Human Adipocytes. *Clinical Infectious Diseases* 71, e549–e560. <https://doi.org/10.1093/cid/ciaa259>
- Gouma, E., Simos, Y., Verginadis, I., Lykoudis, E., Evangelou, A., Karkabounas, S., 2012. A simple procedure for estimation of total body surface area and determination of a new value of Meeh's constant in rats. *Laboratory Animals* 46, 40–45. <https://doi.org/10.1258/la.2011.011021>
- Greene, C., Hanley, N., Campbell, M., 2019. Claudin-5: gatekeeper of neurological function. *Fluids Barriers CNS* 16, 3. <https://doi.org/10.1186/s12987-019-0123-z>
- Grinspoon, S., Carr, A., 2005. Cardiovascular Risk and Body-Fat Abnormalities in HIV-Infected Adults. *The New England Journal of Medicine* 15.
- Guidance for Industry Developing Products for Weight Management, 2007. . *Weight Management* 19.
- Hailu, W., Tesfaye, T., Tadesse, A., 2021. Hyperglycemia After Dolutegravir-Based Antiretroviral Therapy. *IMCRJ* Volume 14, 503–507. <https://doi.org/10.2147/IMCRJ.S323233>
- Hawkins, B.T., Lundeen, T.F., Norwood, K.M., Brooks, H.L., Egleton, R.D., 2007. Increased blood–brain barrier permeability and altered tight junctions in experimental diabetes in the rat: contribution of hyperglycaemia and matrix metalloproteinases 10.
- Herrin, M., Tate, J.P., Akgün, K.M., Butt, A.A., Crothers, K., Freiberg, M.S., Gibert, C.L., Leaf, D.A., Rimland, D., Rodriguez-Barradas, M.C., Ruser, C.B., Herold, K.C., Justice, A.C., 2016. Weight Gain and Incident Diabetes Among HIV-Infected Veterans Initiating Antiretroviral Therapy Compared With Uninfected Individuals. *JAIDS Journal of Acquired Immune Deficiency Syndromes* 73, 228–236. <https://doi.org/10.1097/QAI.0000000000001071>

- Hill, A., Waters, L., Pozniak, A., 2019. Are new antiretroviral treatments increasing the risks of clinical obesity? *Journal of Virus Eradication* 5, 41–43. [https://doi.org/10.1016/S2055-6640\(20\)30277-6](https://doi.org/10.1016/S2055-6640(20)30277-6)
- Hill, A.M., Mitchell, N., Hughes, S., Pozniak, A.L., 2018. Risks of cardiovascular or central nervous system adverse events and immune reconstitution inflammatory syndrome, for dolutegravir versus other antiretrovirals: meta-analysis of randomized trials. *Current Opinion in HIV and AIDS* 13, 102–111. <https://doi.org/10.1097/COH.0000000000000445>
- Hirase, T., Staddon, J.M., Saitou, M., Ando-Akatsuka, Y., Itoh, M., Furuse, M., Fujimoto, K., Tsukita, S., Rubin, L.L., 1997. Occludin as a possible determinant of tight junction permeability in endothelial cells. *Journal of Cell Science* 110, 1603–1613. <https://doi.org/10.1242/jcs.110.14.1603>
- Hirigo, A.T., Gutema, S., Eifa, A., Ketema, W., 2022. Experience of dolutegravir-based antiretroviral treatment and risks of diabetes mellitus. *SAGE Open Medical Case Reports* 10, 2050313X2210794. <https://doi.org/10.1177/2050313X221079444>
- Hoareau, M., El Kholti, N., Debret, R., Lambert, E., 2022. Zebrafish as a Model to Study Vascular Elastic Fibers and Associated Pathologies. *IJMS* 23, 2102. <https://doi.org/10.3390/ijms23042102>
- Hocqueloux, L., Raffi, F., Prazuck, T., Bernard, L., Sunder, S., Esnault, J.-L., Rey, D., Le Moal, G., Roncato-Saberan, M., André, M., Billaud, E., Valéry, A., Avettand-Fènoël, V., Parienti, J.-J., Allavena, C., MONCAY study group, Bollengier-Stragier, O., Esnault, J.-L., Guimard, T., Leautez, S., Perré, P., Lemarie, R., Pouget-Abadie, X., Roncato-Saberan, M., André, M., May, T., Schvoerer, E., Allavena, C., Andre-Garnier, E., Bernaud, C., Billaud, E., Bouchez, S., Hall, N., Raffi, F., Reliquet, V., Vivrel, F., Deleplanque, P., Dos-Santos, A., Sunder, S., Boulard, C., Despujols, A., Guinard, J., Hocqueloux, L., Lefeuvre, S., Mille, C., Niang, M., Ouezzani, M., Prazuck, T., Thomas, G., Valéry, A., Avettand-Fènoël, V., Giraudeau, G., Le Moal, G., Batard, M.-L., Fafi-Kremer, S., Rey, D., Barin, F., Bastides, F., Bernard, L., Gras, G., Hallouin-Bernard, M.C., Lemaigen, A., Le Bret, P., Stefic, K., 2019. Dolutegravir Monotherapy Versus Dolutegravir/Abacavir/Lamivudine for Virologically Suppressed People Living With Chronic Human Immunodeficiency Virus Infection: The Randomized Noninferiority MONotherapy of TiviCAY Trial. *Clinical Infectious Diseases* 69, 1498–1505. <https://doi.org/10.1093/cid/ciy1132>
- Hoffmann, C., Llibre, J.M., 2019. Neuropsychiatric Adverse Events with Dolutegravir and Other Integrase Strand Transfer Inhibitors. *AIDSRev* 21, 1768. <https://doi.org/10.24875/AIDSRev.19000023>

- Hoffmann, C., Welz, T., Sabranski, M., Kolb, M., Wolf, E., Stellbrink, H.-J., Wyen, C., 2017. Higher rates of neuropsychiatric adverse events leading to dolutegravir discontinuation in women and older patients. *HIV Med* 18, 56–63. <https://doi.org/10.1111/hiv.12468>
- Hu, N., Yost, H.J., Clark, E.B., 2001. Cardiac morphology and blood pressure in the adult zebrafish. *Anat. Rec.* 264, 1–12. <https://doi.org/10.1002/ar.1111>
- Jay Widmer, R., Lerman, A., 2014. Endothelial dysfunction and cardiovascular disease. *Global Cardiology Science and Practice* 2014, 43. <https://doi.org/10.5339/gcsp.2014.43>
- Jia, T., Wang, C., Han, Z., Wang, X., Ding, M., Wang, Q., 2020. Experimental Rodent Models of Cardiovascular Diseases. *Front. Cardiovasc. Med.* 7, 588075. <https://doi.org/10.3389/fcvm.2020.588075>
- Kandel, C., Walmsley, S., 2015. Dolutegravir – a review of the pharmacology, efficacy, and safety in the treatment of HIV. *DDDT* 3547. <https://doi.org/10.2147/DDDT.S84850>
- Kirk, J., Plumb, J., Mirakhur, M., McQuaid, S., 2003. Tight junctional abnormality in multiple sclerosis white matter affects all calibres of vessel and is associated with blood-brain barrier leakage and active demyelination. *J. Pathol.* 201, 319–327. <https://doi.org/10.1002/path.1434>
- Kolakowska, A., Maresca, A.F., Collins, I.J., Cailhol, J., 2019. Update on Adverse Effects of HIV Integrase Inhibitors. *Curr Treat Options Infect Dis* 11, 372–387. <https://doi.org/10.1007/s40506-019-00203-7>
- Komarova, Y.A., Kruse, K., Mehta, D., Malik, A.B., 2017. Protein Interactions at Endothelial Junctions and Signaling Mechanisms Regulating Endothelial Permeability. *Circ Res* 120, 179–206. <https://doi.org/10.1161/CIRCRESAHA.116.306534>
- Korencak, M., Byrne, M., Richter, E., Schultz, B.T., Juszczak, P., Ake, J.A., Ganesan, A., Okulicz, J.F., Robb, M.L., de los Reyes, B., Winning, S., Fandrey, J., Burgess, T.H., Esser, S., Michael, N.L., Agan, B.K., Streeck, H., 2019. Effect of HIV infection and antiretroviral therapy on immune cellular functions. *JCI Insight* 4, e126675. <https://doi.org/10.1172/jci.insight.126675>
- Kovacs, L., Kress, T.C., Belin de Chantemèle, E.J., 2022. HIV, Combination Antiretroviral Therapy, and Vascular Diseases in Men and Women. *JACC: Basic to Translational Science* S2452302X21003582. <https://doi.org/10.1016/j.jacbts.2021.10.017>
- Kumar, S., Samaras, K., 2018. The Impact of Weight Gain During HIV Treatment on Risk of Pre-diabetes, Diabetes Mellitus, Cardiovascular Disease, and Mortality. *Front. Endocrinol.* 9, 705. <https://doi.org/10.3389/fendo.2018.00705>
- Lagendijk, A.K., Yap, A.S., Hogan, B.M., 2014. Endothelial cell–cell adhesion during zebrafish vascular development. *Cell Adhesion & Migration* 8, 136–145. <https://doi.org/10.4161/cam.28229>

- Lamorde, M., Atwiine, M., Owarwo, N.C., Ddungu, A., Laker, E.O., Mubiru, F., Kiragga, A., Lwanga, I.B., Castelnovo, B., 2020. Dolutegravir-associated hyperglycaemia in patients with HIV. *The Lancet HIV* 7, e461–e462. [https://doi.org/10.1016/S2352-3018\(20\)30042-4](https://doi.org/10.1016/S2352-3018(20)30042-4)
- Letendre, S.L., Mills, A.M., Tashima, K.T., Thomas, D.A., Min, S.S., Chen, S., Song, I.H., Piscitelli, S.C., on behalf of the extended ING116070 study team, 2014a. ING116070: A Study of the Pharmacokinetics and Antiviral Activity of Dolutegravir in Cerebrospinal Fluid in HIV-1-Infected, Antiretroviral Therapy-Naive Subjects. *Clinical Infectious Diseases* 59, 1032–1037. <https://doi.org/10.1093/cid/ciu477>
- Letendre, S.L., Mills, A.M., Tashima, K.T., Thomas, D.A., Min, S.S., Chen, S., Song, I.H., Piscitelli, S.C., on behalf of the extended ING116070 study team, 2014b. ING116070: A Study of the Pharmacokinetics and Antiviral Activity of Dolutegravir in Cerebrospinal Fluid in HIV-1-Infected, Antiretroviral Therapy-Naive Subjects. *Clinical Infectious Diseases* 59, 1032–1037. <https://doi.org/10.1093/cid/ciu477>
- Li, Y., Wang, C., Zhang, L., Chen, B., Mo, Y., Zhang, J., 2022. Claudin-5a is essential for the functional formation of both zebrafish blood-brain barrier and blood-cerebrospinal fluid barrier. *Fluids Barriers CNS* 19, 40. <https://doi.org/10.1186/s12987-022-00337-9>
- Liu, Y.-Z., Wang, Y.-X., Jiang, C.-L., 2017. Inflammation: The Common Pathway of Stress-Related Diseases. *Front. Hum. Neurosci.* 11, 316. <https://doi.org/10.3389/fnhum.2017.00316>
- Ma, Q., Schifitto, G., Venuto, C., Ocque, A., Dewhurst, S., Morse, G.D., Aalinkeel, R., Schwartz, S.A., Mahajan, S.D., 2020. Effect of Dolutegravir and Sertraline on the Blood Brain Barrier (BBB). *J Neuroimmune Pharmacol* 15, 7–9. <https://doi.org/10.1007/s11481-020-09904-z>
- Makki, K., Froguel, P., Wolowczuk, I., 2013a. Adipose Tissue in Obesity-Related Inflammation and Insulin Resistance: Cells, Cytokines, and Chemokines. *ISRN Inflammation* 2013, 1–12. <https://doi.org/10.1155/2013/139239>
- Makki, K., Froguel, P., Wolowczuk, I., 2013b. Adipose Tissue in Obesity-Related Inflammation and Insulin Resistance: Cells, Cytokines, and Chemokines. *ISRN Inflammation* 2013, 1–12. <https://doi.org/10.1155/2013/139239>
- Massarsky, A., Kozal, J.S., Di Giulio, R.T., 2017. Glutathione and zebrafish: Old assays to address a current issue. *Chemosphere* 168, 707–715. <https://doi.org/10.1016/j.chemosphere.2016.11.004>
- Matsuda, M., Shimomura, I., 2013. Increased oxidative stress in obesity: Implications for metabolic syndrome, diabetes, hypertension, dyslipidemia, atherosclerosis, and cancer. *Obesity Research & Clinical Practice* 7, e330–e341. <https://doi.org/10.1016/j.orcp.2013.05.004>

- McLaughlin, M., Walsh, S., Galvin, S., 2018. Dolutegravir-induced hyperglycaemia in a patient living with HIV. *Journal of Antimicrobial Chemotherapy* 73, 258–260. <https://doi.org/10.1093/jac/dkx365>
- McMahon, C., Trevaskis, J.L., Carter, C., Holsapple, K., White, K., Das, M., Collins, S., Martin, H., Burns-Naas, L.A., 2020. Lack of an association between clinical INSTI-related body weight gain and direct interference with MC4 receptor (MC4R), a key central regulator of body weight. *PLoS ONE* 15, e0229617. <https://doi.org/10.1371/journal.pone.0229617>
- Medina-Leyte, D.J., Zepeda-García, O., Domínguez-Pérez, M., González-Garrido, A., Villarreal-Molina, T., Jacobo-Albavera, L., 2021. Endothelial Dysfunction, Inflammation and Coronary Artery Disease: Potential Biomarkers and Promising Therapeutical Approaches. *IJMS* 22, 3850. <https://doi.org/10.3390/ijms22083850>
- Menard, A., Meddeb, L., Tissot-Dupont, H., Ravoux, I., Dhiver, C., Mokhtari, S., Tomei, C., Brouqui, P., Colson, P., Stein, A., 2017. Dolutegravir and weight gain: an unexpected bothering side effect? *AIDS* 31, 1499–1500. <https://doi.org/10.1097/QAD.0000000000001495>
- Méndez, I., Vázquez-Cuevas, F., Muñoz, R.H., Valente-Godínez, H., Vázquez-Martínez, O., Díaz-Muñoz, M., 2017. Redox Reactions in the Physiopathology of the Liver, in: Khalid, M.A.A. (Ed.), *Redox - Principles and Advanced Applications*. InTech. <https://doi.org/10.5772/intechopen.68841>
- Miano, J.M., Georger, M.A., Rich, A., Bentley, K.L.D.M., 2006. Ultrastructure of Zebrafish Dorsal Aortic Cells. *Zebrafish* 3, 455–463. <https://doi.org/10.1089/zeb.2006.3.455>
- Michel, M., Page-McCaw, P.S., Chen, W., Cone, R.D., 2016. Leptin signaling regulates glucose homeostasis, but not adipostasis, in the zebrafish. *Proc. Natl. Acad. Sci. U.S.A.* 113, 3084–3089. <https://doi.org/10.1073/pnas.1513212113>
- Min, S., Sloan, L., DeJesus, E., Hawkins, T., McCurdy, L., Song, I., Stroder, R., Chen, S., Underwood, M., Fujiwara, T., Piscitelli, S., Lalezari, J., 2011. Antiviral activity, safety, and pharmacokinetics/pharmacodynamics of dolutegravir as 10-day monotherapy in HIV-1-infected adults. *AIDS* 25, 1737–1745. <https://doi.org/10.1097/QAD.0b013e32834a1dd9>
- Mitchell, I.C., Brown, T.S., Terada, L.S., Amatruda, J.F., Nwariaku, F.E., 2010. Effect of Vascular Cadherin Knockdown on Zebrafish Vasculature during Development. *PLoS ONE* 5, 10.
- Montenegro-Burke, J.R., Woldstad, C.J., Fang, M., Bade, A.N., McMillan, J., Edagwa, B., Boska, M.D., Gendelman, H.E., Siuzdak, G., 2019a. Nanoformulated Antiretroviral Therapy Attenuates Brain Metabolic Oxidative Stress. *Mol Neurobiol* 56, 2896–2907. <https://doi.org/10.1007/s12035-018-1273-8>

- Montenegro-Burke, J.R., Woldstad, C.J., Fang, M., Bade, A.N., McMillan, J., Edagwa, B., Boska, M.D., Gendelman, H.E., Siuzdak, G., 2019b. Nanoformulated Antiretroviral Therapy Attenuates Brain Metabolic Oxidative Stress. *Mol Neurobiol* 56, 2896–2907. <https://doi.org/10.1007/s12035-018-1273-8>
- Montero-Balaguer, M., Swirsding, K., Orsenigo, F., Cotelli, F., Mione, M., Dejana, E., 2009. Stable Vascular Connections and Remodeling Require Full Expression of VE-Cadherin in Zebrafish Embryos. *PLoS ONE* 4, e5772. <https://doi.org/10.1371/journal.pone.0005772>
- Mulhem, A., Moulla, Y., Klötting, N., Ebert, T., Tönjes, A., Fasshauer, M., Dietrich, A., Schön, M.R., Stumvoll, M., Richter, V., Blüher, M., 2021. Circulating cell adhesion molecules in metabolically healthy obesity. *Int J Obes* 45, 331–336. <https://doi.org/10.1038/s41366-020-00667-4>
- Musekwa, R., Hamooya, B.M., Koethe, J.R., Nzala, S., Masenga, S.K., 2021. Prevalence and correlates of hypertension in HIV-positive adults from the Livingstone Central Hospital, Zambia. *Pan Afr Med J* 39. <https://doi.org/10.11604/pamj.2021.39.237.29718>
- Myers, M.G., Leibel, R.L., Seeley, R.J., Schwartz, M.W., 2010. Obesity and leptin resistance: distinguishing cause from effect. *Trends in Endocrinology & Metabolism* 21, 643–651. <https://doi.org/10.1016/j.tem.2010.08.002>
- Nair, A., Jacob, S., 2016. A simple practice guide for dose conversion between animals and human. *J Basic Clin Pharma* 7, 27. <https://doi.org/10.4103/0976-0105.177703>
- Nkeh-Chungag, B.N., Goswami, N., Engwa, G.A., Sewani-Rusike, C.R., Mbombela, V., Webster, I., De Boever, P., Kessler, H.H., Stelzl, E., Strijdom, H., 2021. Relationship between Endothelial Function, Antiretroviral Treatment and Cardiovascular Risk Factors in HIV Patients of African Descent in South Africa: A Cross-Sectional Study. *JCM* 10, 392. <https://doi.org/10.3390/jcm10030392>
- Norwood, J., Turner, M., Bofill, C., Rebeiro, P., Shepherd, B., Bebawy, S., Hulgan, T., Raffanti, S., Haas, D.W., Sterling, T.R., Koethe, J.R., 2018. Weight Gain in Persons with HIV Switched from Efavirenz-based to Integrase Strand Transfer Inhibitor-based Regimens 10.
- Nwariaku, F.E., Liu, Z., Zhu, X., Nahari, D., Ingle, C., Wu, R.F., Gu, Y., Sarosi, G., Terada, L.S., 2004. NADPH oxidase mediates vascular endothelial cadherin phosphorylation and endothelial dysfunction. *Blood* 104, 3214–3220. <https://doi.org/10.1182/blood-2004-05-1868>
- Oka, T., Nishimura, Y., Zang, L., Hirano, M., Shimada, Y., Wang, Z., Umemoto, N., Kuroyanagi, J., Nishimura, N., Tanaka, T., 2010. Diet-induced obesity in zebrafish shares common pathophysiological pathways with mammalian obesity. *BMC Physiol* 10, 21. <https://doi.org/10.1186/1472-6793-10-21>

- Okello, S., Kanyesigye, M., Muyindike, W.R., Annex, B.H., Hunt, P.W., Haneuse, S., Siedner, M.J., 2015. Incidence and predictors of hypertension in adults with HIV-initiating antiretroviral therapy in south-western Uganda. *Journal of Hypertension* 33, 2039–2045. <https://doi.org/10.1097/HJH.0000000000000657>
- Omran, F., Christian, M., 2020. Inflammatory Signaling and Brown Fat Activity. *Front. Endocrinol.* 11, 156. <https://doi.org/10.3389/fendo.2020.00156>
- Pai, M.P., 2012. Drug dosing based on weight and body surface area: Mathematical assumptions and limitations in obese adults. *Pharmacotherapy* 32, 856–868. <https://doi.org/10.1002/j.1875-9114.2012.01108.x>
- Pizzi, C., Mancini, S., Angeloni, L., Fontana, F., Manzoli, L., Costa, G.M., 2009. Effects of Selective Serotonin Reuptake Inhibitor Therapy on Endothelial Function and Inflammatory Markers in Patients With Coronary Heart Disease. *Clin Pharmacol Ther* 86, 527–532. <https://doi.org/10.1038/clpt.2009.121>
- Rajendran, P., Rengarajan, T., Thangavel, J., Nishigaki, Y., Sakthisekaran, D., Sethi, G., Nishigaki, I., 2013. The Vascular Endothelium and Human Diseases. *Int. J. Biol. Sci.* 9, 1057–1069. <https://doi.org/10.7150/ijbs.7502>
- Rameshrad, M., Babaei, H., Azarmi, Y., Fouladi, D.F., 2016. Rat aorta as a pharmacological tool for in vitro and in vivo studies. *Life Sciences* 145, 190–204. <https://doi.org/10.1016/j.lfs.2015.12.043>
- Rao, R., 2008. Oxidative stress-induced disruption of epithelial and endothelial tight junctions. *Front Biosci Volume*, 7210. <https://doi.org/10.2741/3223>
- Rao, R.K., Basuroy, S., Rao, V.U., Karnaky, K.J., Gupta, A., 2002. Tyrosine phosphorylation and dissociation of occludin–ZO-1 and E-cadherin– β -catenin complexes from the cytoskeleton by oxidative stress. *Biochemical Journal* 368, 471–481. <https://doi.org/10.1042/bj20011804>
- Rea, I.M., Gibson, D.S., McGilligan, V., McNerlan, S.E., Alexander, H.D., Ross, O.A., 2018. Age and Age-Related Diseases: Role of Inflammation Triggers and Cytokines. *Front. Immunol.* 9, 586. <https://doi.org/10.3389/fimmu.2018.00586>
- Reagan-Shaw, S., Nihal, M., Ahmad, N., 2008. Dose translation from animal to human studies revisited. *FASEB j.* 22, 659–661. <https://doi.org/10.1096/fj.07-9574LSF>
- Reglero-Real, N., Colom, B., Bodkin, J.V., Nourshargh, S., 2016. Endothelial Cell Junctional Adhesion Molecules: Role and Regulation of Expression in Inflammation. *Arterioscler Thromb Vasc Biol.* 36, 2048–2057. <https://doi.org/10.1161/ATVBAHA.116.307610>
- Ronson, R., 1999. The cardiovascular effects and implications of peroxynitrite. *Cardiovascular Research* 44, 47–59. [https://doi.org/10.1016/S0008-6363\(99\)00184-4](https://doi.org/10.1016/S0008-6363(99)00184-4)
- Sax, P.E., Erlandson, K.M., Lake, J.E., Mcomsey, G.A., Orkin, C., Esser, S., Brown, T.T., Rockstroh, J.K., Wei, X., Carter, C.C., Zhong, L., Brainard, D.M., Melbourne, K., Das,

- M., Stellbrink, H.-J., Post, F.A., Waters, L., Koethe, J.R., 2020. Weight Gain Following Initiation of Antiretroviral Therapy: Risk Factors in Randomized Comparative Clinical Trials. *Clinical Infectious Diseases* 71, 1379–1389. <https://doi.org/10.1093/cid/ciz999>
- Schouten, J., Cinque, P., Gisslen, M., Reiss, P., Portegies, P., 2011. HIV-1 infection and cognitive impairment in the cART era: a review. *AIDS* 25, 561–575. <https://doi.org/10.1097/QAD.0b013e3283437f9a>
- Schwayer, C., Shamipour, S., Pranjic-Ferscha, K., Schauer, A., Balda, M., Tada, M., Matter, K., Heisenberg, C.-P., 2019. Mechanosensation of Tight Junctions Depends on ZO-1 Phase Separation and Flow. *Cell* 179, 937-952.e18. <https://doi.org/10.1016/j.cell.2019.10.006>
- Sculier, D., Doco-Lecompte, T., Yerly, S., Metzner, K., Decosterd, L., Calmy, A., 2018. Stable HIV-1 reservoirs on dolutegravir maintenance monotherapy: the MONODO study. *HIV Med* 19, 572–577. <https://doi.org/10.1111/hiv.12626>
- Shah, A., Gangwani, M.R., Chaudhari, N.S., Glazyrin, A., Bhat, H.K., Kumar, A., 2016. Neurotoxicity in the Post-HAART Era: Caution for the Antiretroviral Therapeutics. *Neurotox Res* 30, 677–697. <https://doi.org/10.1007/s12640-016-9646-0>
- Snijder, M.B., Dekker, J.M., Visser, M., Bouter, L.M., Stehouwer, C.D., Kostense, P.J., Yudkin, J.S., Heine, R.J., Nijpels, G., Seidell, J.C., 2003. Associations of hip and thigh circumferences independent of waist circumference with the incidence of type 2 diabetes: the Hoorn Study. *The American Journal of Clinical Nutrition* 77, 1192–1197. <https://doi.org/10.1093/ajcn/77.5.1192>
- Song, Y., Cone, R.D., 2007. Creation of a genetic model of obesity in a teleost. *FASEB j.* 21, 2042–2049. <https://doi.org/10.1096/fj.06-7503com>
- Storch, A.S., Mattos, J.D. de, Alves, R., Galdino, I. dos S., Rocha, H.N.M., 2017. Methods of Endothelial Function Assessment: Description and Applications. *International Journal of Cardiovascular Sciences*. <https://doi.org/10.5935/2359-4802.20170034>
- Thivalapill, N., Simelane, T., Mthethwa, N., Dlamini, S., Lukhele, B., Okello, V., Kirchner, H.L., Mandalakas, A.M., Kay, A.W., 2021. Transition to Dolutegravir Is Associated With an Increase in the Rate of Body Mass Index Change in a Cohort of Virally Suppressed Adolescents. *Clinical Infectious Diseases* 73, e580–e586. <https://doi.org/10.1093/cid/ciaa1652>
- Triant, V.A., 2013. Cardiovascular Disease and HIV Infection. *Curr HIV/AIDS Rep* 10, 199–206. <https://doi.org/10.1007/s11904-013-0168-6>
- Trickey, A., May, M.T., Vehreschild, J.-J., Obel, N., Gill, M.J., Crane, H.M., Boesecke, C., Patterson, S., Grabar, S., Cazanave, C., Cavassini, M., Shepherd, L., Monforte, A. d'Arminio, van Sighem, A., Saag, M., Lampe, F., Hernando, V., Montero, M., Zangerle, R., Justice, A.C., Sterling, T., Ingle, S.M., Sterne, J.A.C., 2017. Survival of HIV-positive

- patients starting antiretroviral therapy between 1996 and 2013: a collaborative analysis of cohort studies. *The Lancet HIV* 4, e349–e356. [https://doi.org/10.1016/S2352-3018\(17\)30066-8](https://doi.org/10.1016/S2352-3018(17)30066-8)
- U.S Department of Health and Human Services, Food and Drug Administration, Center for Drug Evaluation and Research (CDER), Center for Biologics Evaluation and Research (CBER), Oncology Center of Excellence (OCE), 2019. Considerations for the Inclusion of Adolescent Patients in Adult Oncology Clinical Trials Guidance for Industry.
- van Leeuwen, L.M., Evans, R.J., Jim, K.K., Verboom, T., Fang, X., Bojarczuk, A., Malicki, J., Johnston, S.A., van der Sar, A.M., 2018. A transgenic zebrafish model for the *in vivo* study of the blood and choroid plexus brain barriers using *claudin 5*. *Biology Open* 7, bio030494. <https://doi.org/10.1242/bio.030494>
- van Lunzen, J., Maggiolo, F., Arribas, J.R., Rakhmanova, A., Yeni, P., Young, B., Rockstroh, J.K., Almond, S., Song, I., Brothers, C., Min, S., 2012. Once daily dolutegravir (S/GSK1349572) in combination therapy in antiretroviral-naive adults with HIV: planned interim 48 week results from SPRING-1, a dose-ranging, randomised, phase 2b trial. *The Lancet Infectious Diseases* 12, 111–118. [https://doi.org/10.1016/S1473-3099\(11\)70290-0](https://doi.org/10.1016/S1473-3099(11)70290-0)
- Venter, W.D.F., Moorhouse, M., Sokhela, S., Fairlie, L., Mashabane, N., Masenya, M., Serenata, C., Akpomiemie, G., Qavi, A., Chandiwana, N., Norris, S., Chersich, M., Clayden, P., Abrams, E., Arulappan, N., Vos, A., McCann, K., Simmons, B., Hill, A., 2019. Dolutegravir plus Two Different Prodrugs of Tenofovir to Treat HIV. *N Engl J Med* 381, 803–815. <https://doi.org/10.1056/NEJMoa1902824>
- Weyer, C., Foley, J.E., Bogardus, C., Tataranni, P.A., Pratley, R.E., 2000. Enlarged subcutaneous abdominal adipocyte size, but not obesity itself, predicts Type II diabetes independent of insulin resistance. *Diabetologia* 43, 1498–1506. <https://doi.org/10.1007/s001250051560>
- Wijting, I., Rokx, C., Boucher, C., van Kampen, J., Pas, S., de Vries-Sluijs, T., Schurink, C., Bax, H., Derksen, M., Andrinopoulou, E.-R., van der Ende, M., van Gorp, E., Nouwen, J., Verbon, A., Bierman, W., Rijnders, B., 2017. Dolutegravir as maintenance monotherapy for HIV (DOMONO): a phase 2, randomised non-inferiority trial. *The Lancet HIV* 4, e547–e554. [https://doi.org/10.1016/S2352-3018\(17\)30152-2](https://doi.org/10.1016/S2352-3018(17)30152-2)
- World Health Organization, 2016. World health statistics 2016: monitoring health for the SDGs, sustainable development goals. World Health Organization, Geneva.
- Xiangdong, L., Yuanwu, L., Hua, Z., Liming, R., Qiuyan, L., Ning, L., 2011. Animal models for the atherosclerosis research: a review. *Protein Cell* 2, 189–201. <https://doi.org/10.1007/s13238-011-1016-3>

- Yang, Z., Wu, S., Fontana, F., Li, Y., Xiao, W., Gao, Z., Stephan, A., Affolter, M., Belting, H.-G., Abdelilah-Seyfried, S., Zhang, J., 2020. The tight junctions protein Claudin-5 limits endothelial cell motility. *Journal of Cell Science* jcs.248237. <https://doi.org/10.1242/jcs.248237>
- Zakumumpa, H., Kitutu, F.E., Ndagije, H.B., Diana, N.-K., Ssanyu, J.N., Kiguba, R., 2021. Provider perspectives on the acceptability and tolerability of dolutegravir-based anti-retroviral therapy after national roll-out in Uganda: a qualitative study. *BMC Infect Dis* 21, 1222. <https://doi.org/10.1186/s12879-021-06933-8>
- Zang, L., Maddison, L.A., Chen, W., 2018. Zebrafish as a Model for Obesity and Diabetes. *Front. Cell Dev. Biol.* 6, 91. <https://doi.org/10.3389/fcell.2018.00091>
- Zang, L., Shimada, Y., Nishimura, N., 2017. Development of a Novel Zebrafish Model for Type 2 Diabetes Mellitus. *Sci Rep* 7, 1461. <https://doi.org/10.1038/s41598-017-01432-w>

7. LIST OF APPENDICES

7.1. Appendix A Zebrafish study ethical approval document.



UNIVERSITEIT
STELLENBOSCH
UNIVERSITY

Protocol Approval

Date: 26 June 2021

PI Name: Miss J Conradie

Protocol #: ACU-2021-21999

Title: The effect of Dolutegravir on overall vascular oxidative and inflammatory profile.

Dear J Conradie ,

Your response to modifications, was reviewed by the Research Ethics Committee: Animal Care and Use via committee review procedures and was approved. Please note that this clearance is only valid for a period of twelve months. Ethics clearance of protocols spanning more than one year must be renewed annually through submission of a progress report, up to a maximum of three years.

Approval Date: **24 June 2021 - 23 June 2022**

Animal Species: **Danio Rerio (Zebrafish)**

Animal Numbers: **48**

Applicants are reminded that they are expected to comply with accepted standards for the use of animals in research and teaching as reflected in the South African National Standards 10386: 2008. The SANS 10386: 2008 document is available on the Division for Research Developments website www.sun.ac.za/research.

As provided for in the Veterinary and Para-Veterinary Professions Act, 1982. It is the principal investigator's responsibility to ensure that all study participants are registered with or have been authorised by the South African Veterinary Council (SAVC) to perform the procedures on animals, or will be performing the procedures under the direct and continuous supervision of a SAVC-registered veterinary professional or SAVC-registered para-veterinary professional, who are acting within the scope of practice for their profession.

Please remember to use your protocol number 21999 on any documents or correspondence with the REC: ACU concerning your research protocol.

Please note that the REC: ACU has the prerogative and authority to ask further questions, seek additional information, require further modifications or monitor the conduct of your research.

Any event not consistent with routine expected outcomes that results in any unexpected animal welfare issue (death, disease, or prolonged distress) or human health risks (zoonotic disease or exposure, injuries) must be reported to the committee, by creating an Adverse Event submission within the system.

We wish you the best as you conduct your research.

If you have any questions or need further help, please contact the REC: ACU Secretariat at wabeukes@sun.ac.za or 021 808 9003.

Sincerely,

Winston Beukes

REC: ACU Secretariat

Research Ethics Committee: Animal Care and Use

7.2. Appendix B

Rat study ethical approval document.



Approved with Stipulations

24/06/2021

PI: Dr KS Petersen-Ross

REC: ACU Reference #: ACU-2021-22035

Title: Obesity; a confounder in Dolutegravir treatment?

Dear Dr KS Petersen-Ross

Your response to modifications, with reference number #ACU-2021-22035 was reviewed by the Research Ethics Committee: Animal Care and Use via committee review procedures and was approved on condition that the following stipulations are clarified:

1. A long list of side effects and adverse clinical effects to the drug that will be given is provided; however, the pain and distress category is given as C. Will the animals not require treatment or intervention if they develop these symptoms?
2. Rats will be housed 4 per cage and be given jelly blocks for the drug administration. How will you ensure that each rat get the same amount of drugs?

Applicants are reminded that they are expected to comply with accepted standards for the use of animals in research and teaching as reflected in the South African National Standards 10386: 2008. The SANS 10386: 2008 document is available on the Division for Research Developments website www.sun.ac.za/research.

As provided for in the Veterinary and Para-Veterinary Professions Act, 1982. It is the principal investigator's responsibility to ensure that all study participants are registered with or have been authorised by the South African Veterinary Council (SAVC) to perform the procedures on animals, or will be performing the procedures under the direct and continuous supervision of a SAVC-registered veterinary professional or SAVC-registered para-veterinary professional, who are acting within the scope of practice for their profession.

Please remember to use your REC: ACU reference number: # ACU-2021-22035 on any documents or correspondence with the REC: ACU concerning your research protocol.

If you have any questions or need further help, please contact the REC: ACU office at 021 808 9003.

Visit the Division for Research Developments website www.sun.ac.za/research for documentation on REC: ACU policy and procedures.

Sincerely,

Mr Winston Beukes

Coordinator: Research Ethics (Animal Care and Use)

7.3. Appendix C

Hikari micro pellets composition

Table 7.1: The amount of the constituents found in Hikari micro pellets.

Constituents	Amount
Crude Protein	min. 43%
Crude Fat	min. 7.0%
Crude Fibre	min. 7.0%
Moisture	max 10%
Ash	max 17%
Phosphorus	min 1.1%
Vitamin A	min. 16 000 IU/kg
Vitamin D3	min. 2400 IU/kg
Vitamin E	min. 960 IU/kg
Ascorbic acid	min. 360 mg/kg